



Results

MOLECULAR MODELING & COMPUTATIONAL CHEMISTRY

Vol. 14, No. 3

1 April 2005

Coverage period: 1 Mar. 2005 through 1 April 2005
About 253 papers from 13 journals are cited.

1. APPLICATIONS (105) page 2

1.1 Small Molecules – 29

| | |
|----------------------------|--------------------------|
| Water and Solvation – 6 | QSAR – 12 |
| Med Chem & Drug Design - 9 | Carbon Nanoparticles - 2 |

1.2 Biopolymers – 73

| | |
|----------------------------------|----------------------------|
| Bioinformatics – 6 | Protein Dynamics – 5 |
| Protein Seq Anal and Align – 3 | Ligand Binding – 4 |
| Protein Structure Prediction – 2 | Enzyme Catalysis – 8 |
| Comp and Homol Modeling – 3 | Protein-Protein Inter. – 2 |
| Peptide Conform Anal – 1 | Membrane Proteins - 9 |
| Protein Structure Anal – 8 | Protein Nuc Acid Inter - 1 |
| Protein Folding – 6 | Nucleic Acids – 4 |
| Protein Design& Engineering – 2 | Lipids and Surfactants - 4 |
| Protein Hydration – 3 | Carbohydrates - 1 |
| Protein Electr and Titr – 1 | |

1.3 Polymers – 2

1.4 Surfaces, Catalysts, and Materials Subjects — 1

2. METHODOLOGY (28) page 21

| | |
|--------------------------------|---------------------------|
| QSAR – 2 | Molecular Dynamics – 4 |
| Conformational Search Anal - 1 | Free Energy Methods- 3 |
| Potentials and Parameters – 11 | QM/MM – 2 |
| Boundary Conditions - 1 | Surface/Volume Deter. - 2 |
| Solvation Energy - 2 | |

3. JOURNAL REVIEWS (120) page 26

J. Comp. Chem. **26** (6), 30 April 2005
J. Comp. Chem. **26** (7), May 2005
J. Mol. Modeling **11** (1) Feb 2005
J Am Chem Soc **127** (9-13) 2005
J Chem Theor Comput **1** (2) March 2005
J Phys Chem B **109** (5-13) 2005

4. ADDRESSES OF PRINCIPLE AUTHORS page 38

5. COPYRIGHT, DISCLAIMER AND PUBLISHER INFORMATION

Editorial and News

A groundbreaker in membrane biophysics was published by Gunther Peters and colleagues this month in *J. Chem. Physics* (see **Methodology, Molecular Dynamics**). It deals with a problem in membrane biophysics that has achieved nearly universal interest in the past year or so, the computation of the lateral pressure profile in the lipid bilayer. The reason this is so interesting is the heterogeneous and variable shapes of membrane proteins. Although we still don't know much about them, membrane NMR and spectroscopic studies of membrane proteins are starting to reveal small but significant variations in contour at their interfaces with lipid membranes and large conformational changes during function. Although most membrane proteins are essentially right cylinders (either β -barrels or helix bundles) with axes parallel to the membrane normal, border helices or strands can sometimes have tilts, kinks, or extrusions that require accommodation by bilayer lipids.

The current paper tackles the problem of how to define the local pressure tensor, comparing contour definitions that lead to Irving-Kirkwood or Hiroshima tensors, and showed them to give similar results for the DPPC bilayer. Then they developed a methodology based on the Hiroshima tensor for determining the Ewald sum contribution to the electrostatic component of the local pressure tensor and showed that the results with this new method are similar to those obtained with very long cutoffs. This is important, because for shorter cutoffs, the lateral pressure profile shape was quite sensitive to the cutoff length, undoubtedly due to the heterogeneous nature of the charge distribution near the interface. Hopefully these new methods will become useful tools in the membrane biophysicist's arsenal.

David D. Busath, Editor

1. APPLICATIONS

1.1. *Small Molecules*

Water and Solvation

On the mechanism of hydrophobic association of nanoscopic solutes.

N. Choudhury, and B.M. Pettitt* [U Houston]

J. Amer. Chem. Soc. **127**, 3556-3567 (2005)

Detailed atomistic MD and free energy simulation of hydration between two nanoscopic plates, contradicting previous theoretical predictions, shows a profound dependence on the weak attractive interactions between the solute and the solvent and the solute size.

Accurate prediction of absolute acidity constants in water with a polarizable force field: Substituted phenols, methanol, and imidazole.

G. A. Kaminski* [Central Michigan U]

J. Phys. Chem. B **109**, 5884-5890 (2005)

A force field with inducible point dipoles is tested for its ability to calculate absolute pKa values and compared to a non-additive (OPLS-AA) force field. Proper treatment of the electrostatics, via Ewald, is shown to be important.

Dynamics of water trapped between hydrophobic surfaces.

N. Choudhury, and B.M. Pettitt* [U Houston]

J. Phys. Chem. B **109**, 6422-6429 (2005)


MD simulations explore the dynamic behavior of solvent between two nanoscopic hydrophobic solutes (see the JACS review in this issue).

Phase diagram of water between hydrophobic surfaces.

K. Koga* [Okayama U] and H. Tanaka

J. Chem. Phys. **122**, 10471101-10471106 (2005)

TIP4P water confined between smooth-walled planes forms a monolayer or bilayer of ice with fully connected hydrogen bonding, like in bulk. The bilayer can be either amorphous or crystalline. Here the computed phase diagrams are presented.

| | | |
|---|---|--|
|  <p>MMCC Results David Busath, Ed. 706 Sunny Lane Orem, UT 84058</p> <p>Tel. (801) 422-8753 Fax (801) 422-0700 e-mail: mmcc@itsnet.com</p> <p>David Busath, M.D., Professor, Dept. of Physiology and Dev. Biol. Brigham Young Univ., Provo, UT</p> <p>Editor Emeritus: Bruce Gelin, Ph.D. Dr. Gelin was founder of MMCC Results and edited volumes 1-6.</p> | <p><i>MMCC Results</i> (ISSN 1061-6381) is published ten times per year at the beginning of each month except January and August by the independent business, MMCC Results. Mention of software, hardware, or other products is for informational purposes only and does not constitute an endorsement or recommendation by MMCC Results nor by the authors of the paper cited. All product names are the trademarks or registered symbols of their respective holders.</p> <p>Marginal symbols indicate that the authors acknowledged the use of a software package from a commercial source. A refers to Accelrys Inc. and T to Tripos Inc. Other companies are denoted by their name in a box. Papers of special interest are marked by an exclamation point.</p> <p>Copyright © 2005 MMCC Results</p> | <p>Associate Editor: Thomas Cheatham Univ. of Utah, Salt Lake City, UT</p> <p>Assistant Editors: Alan C. Cheng Pfizer Global R&D, Cambridge, MA</p> <p>Anston Feenstra Vrije Univ., Amsterdam, Netherlands</p> <p>R. Nageswara Ramireddy Genomik Design Pharmaceuticals Pvt. Ltd. Hyderabad, India</p> |
|---|---|--|

Water and Solvation (cont'd)

Computing the Soret coefficient in aqueous mixtures using boundary driven nonequilibrium molecular dynamics.

C. Nieto-Draghi* [U Rovira i Virgili], J.B. Ávalos, and B. Rousseau

J. Chem. Phys. **122**, 11450301-11450308 (2005)

The Soret effect may be valuable for isotope separation. Because of differences in the temperature dependence of diffusion for different molecules, they will separate somewhat in a mixture with an imposed temperature gradient. Nonequilibrium MD simulations show that water-ethanol and water-methanol mixtures show the experimentally observed behavior, the cause being molecular interactions. Aqueous mixtures of acetone and DMSO are predicted to have similar behaviors.

The melting temperature of the most common models of water.

C. Vega* [U Complutense], E. Sanz, and J.L.F. Abascal

J. Chem. Phys. **122**, 11450701-11450709 (2005)

Gibbs-Duhem methodology is applied to examine the effects of water parameters on melting temperature of Ice *h* and stability of Ice *h* relative to Ice II at the melting point. At P=1 bar, SPC, SPC/E, TIP3P, TIP4P, TIP4P/Ew, and TIP5P models melting points are 215 K, 146 K, 232 K, 245 K, and 274 K, respectively. Because of the position of the negative charge along the H-O-H bisector in SPC, SPC/E, TIP3P, and TIP5P, Ice *h* is not stable at the melting point, but Ice II is.

Medicinal Chemistry and Drug Design

Inhibitory effects of 2-substituted-1-naphthol derivatives on cyclooxygenase I and II.

B. Kongkathip, C. Sangma, K. Kirtikara, S. Luangkamin, K. Hasitapan, N. Jongkon, S. Hannongbua and N. Kongkathip* [Kasetsart U]

Bioorg. Med. Chem. **13**, 2167-2175 (2005)

Docking studies indicated that the presence of hydroxyl group at C-1 position on the naphthalene nucleus enhanced the anti-inflammatory activity towards COX-2. C-2' Dimethyl substituents on the propyl chain also increased the inhibitory activity. The results provided a model for the binding of the naphthol derivatives to COX-2 and facilitate the design of more potent or selective analogs prior to synthesis.

Design, synthesis, and biological evaluation of *N*-acetyl-2-carboxybenzenesulfonamides: a novel class of cyclooxygenase-2 (COX-2) inhibitors.

Q.H. Chen, P.N. Praveen Rao and E.E. Knaus* [U Alberta]

Bioorg. Med. Chem. **13**, 2459-2468 (2005)

Molecular Modeling study indicated that the SO₂NHCOCH₃ substituent present in *N*-acetyl-2-carboxy-4-(2,4-fluorophenyl)benzenesulfonamide is suitably positioned to acetylate the Ser⁵³⁰ hydroxyl group in the COX-2 primary binding site. The results showed that the SO₂NHCOCH₃ pharmacophore present in *N*-acetyl-2-carboxybenzenesulfonamides is a suitable bioisostere for the acetoxy (OCOMe) group in aspirin.

A topological substructural approach applied to the computational prediction of rodent carcinogenicity.

A.M. Helguera, M.A.C. Pérez* [Cent U Las Villas], M.P. González, R.M. Ruiz and H.G. Díaz

Bioorg. Med. Chem. **13**, 2477-2488 (2005)

TOPS-MODE approach is used to investigate the carcinogenic and noncarcinogenic activity on a data set of 189 compounds. This methodology evidenced that the hydrophobicity increase the carcinogenic activity and the dipole moment of the molecule decrease it and suggested the capacity of the TOPS-MODE descriptors to estimate this property for new drug candidates.

 Medicinal Chemistry and Drug Design (cont'd)

Tetracycline and its analogues as inhibitors of amyloid fibrils: searching for a geometrical pharmacophore by theoretical investigation of their conformational behavior in aqueous solution.

U. Cosentino, M. Rosaria-Vari, A.A.G. Saracino, D. Pitea, G. Moro* [U Sudi di Milano-Bicocca] and M. Salmona

J. Mol. Mod. **11**, 17-25 (2005)

Geometrical pharmacophore is used to investigate the relationship between conformational flexibility and biological activity in aqueous solution, the conformational behavior of 15 TCs in both the zwitterionic and the anionic forms. An *extended* and a *folded* conformation characterized by different intramolecular hydrogen-bond networks were found in Tetracycline. TC properties other than geometrical ones have a crucial role in determining their anti-fibrillogenic ability.

!

Generation of multiple pharmacophore hypotheses using multiobjective optimisation techniques.

S.J. Cottrell, V.J. Gillet* [U Sheffield], R. Taylor, and D.J. Wilton

J. Comput.-Aid. Molec. Design **18**, 665-682 (2004)

A novel pharmacophore-generating algorithm is presented, that explores conformations on the fly, and aims to present several plausible models for further consideration (instead of just one 'best', or many 'possible' ones). Application to 5-HT_{1D} antagonists, scythalone DH inhibitors and D2 antagonists show that often goodness-of-fit is balanced by internal strain, and strengths and weaknesses with respect to other methods are discussed.

Conformational analysis of methylphenidate: Comparison of molecular orbital and molecular mechanics methods.

K.M. Gilbert, W.J. Skawinski, M. Misra, K.A. Paris, N.H. Naik, R.A. Buono, H.M. Deutsch, and C.A. Venanzi* [New Jersey Inst Tech]

J. Comput.-Aid. Molec. Design **18**, 719-738 (2004)

Comparisons between Triplos MM, AM1 and 6-31G* HF and B3LYP calculations on methylphenidate potential energy surfaces show striking similarities and interesting differences. Effects of inclusion of solvent are analyzed and discussed.

T

Docking studies on NSAID/COX-2 isozyme complexes using Contact Statistics analysis

G. Ermondi* [U Torino], G. Caron, R. Lawrence, and D. Longo

J. Comput.-Aid. Molec. Design **18**, 683-696 (2004)

Docking poses of COX2 inhibitors from two docking methods are ranked on 'plausibility' by the MOE 'contact statistics' comparison with crystal structure contact frequencies, and results are analyzed and compared in detail.

Chem. Comput.

A

Comparison of conformational analysis techniques to generate pharmacophore hypotheses using Catalyst.

R. Kristam, V.J. Gillet* [U Sheffield], R.A. Lewis, and D. Thorner

J. Chem. Inf. Model. **45**, 461-476 (2005)

Comparison of conformation generation programs suggest that rule-based methods are just as good as or better than slower, more rigorous approaches for generation of pharmacophore models in Catalyst. The authors also make suggestions to improve reproducibility of published results.

 Medicinal Chemistry and Drug Design (cont'd)

A shape-based 3-D scaffold hopping method and its application to a bacterial protein-protein interaction.

T.S. Rush III* [Wyeth], J.A. Grant, L. Mosyak, and A. Nicholls

J. Med. Chem. **48**, 1489-1495 (2005)

Weakly binding inhibitors of the antibacterial target ZipA-FtsZ are discovered using a high throughput shape comparison virtual screening program called ROCS.

Quantitative Structure-Activity Relations

Properties and structure-activity studies of cyclic β -hairpin peptidomimetics based on the cationic antimicrobial peptide protegrin I.

J.A. Robinson* [U Zurich], S.C. Shankamma, P. Jetter, U. Kienzl, R.A. Schwendener, D. Obrecht and J.W. Vrijbloed

Bioorg. Med. Chem. **13**, 2055-2064 (2005)

Structural Activity Relationship studies showed that the antimicrobial activity was tolerant to a large number of the substitutions tested. Some analogues showed slightly improved antimicrobial activities, whereas other substitutions caused large increases in haemolytic activity on human red blood cells.

Design, synthesis, antibacterial and QSAR studies of benzimidazole and imidazole chloroaryloxyalkyl derivatives.

A.K. Nezhad* [Shiraz U], M.N. Soltani Rad, Z. Asrari, H. Mohabatkar, and B. Hemmateenejad

Bioorg. Med. Chem. **13**, 1931-1938 (2005)

Different electronic, topologic, functional groups and physicochemical descriptors are calculated for each molecule in QSAR analysis. A three parametric equation was found between the log MIC and HOMO energy, hydration energy and number of primary carbon atoms of the molecules.

Molecular docking and 3D-QSAR studies on the binding mechanism of statine-based peptidomimetics with β -secretase.

Z. Zuo, X. Luo, W. Zhu, J. Shen, X. Shen, H. Jiang* [Chinese Acad Sci] and K. Chen

Bioorg. Med. Chem. **13**, 2121-2131 (2005)

The Lamarckian Genetic Algorithm was applied to locate the binding orientations and conformations of the peptidomimetics with the β -secretase. Both CoMFA and CoMSIA field distributions are in good agreement with the structural characteristics of the binding groove of the β -secretase. 3D-QSAR models and the inhibitor-enzyme interactions are useful in developing new drug leads against Alzheimer's disease.

Structure-activity study of *epi*-gallocatechin gallate (EGCG) analogs as proteasome inhibitors.

S.B. Wan, K.R.L. Piwowar, D.J. Kuhn, D. Chen, Q.P. Dou and T.H. Chan* [Hong Kong Polytech U]

Bioorg. Med. Chem. **13**, 2177-2185 (2005)

In B ring, a decrease in the number of OH groups led to decreased potency. Hydrophobic benzyl group is introducing into the 8 position of A ring has no significant affect on the proteasome-inhibitory potency.

T

Quantitative Structure-Activity Relationships (cont'd)

A physically interpretable quantum-theoretic QSAR for some carbonic anhydrase inhibitors with diverse aromatic rings, obtained by a new QSAR procedure.

B.W. Clare* [U Western Australia] and C.T. Supuran

Bioorg. Med. Chem. **13**, 2197-2211 (2005)

B3LYP/6-31G* level is used for calculations and QSAR models are developed. A significant correlation was obtained with charge on the atoms of the sulfonamide group, followed by the nodal orientation. The solvation energy calculated by COSMO and the charge polarization of the molecule calculated as the mean absolute Mulliken charge over all atoms.

T

Comparative molecular similarity indices analysis (CoMSIA) studies of 1,2-naphthoquinone derivatives as PTP1B inhibitors.

M.E. Sobhia and P.V. Bharatam* [NIPER]

Bioorg. Med. Chem. **13**, 2331-2338 (2005)

Protein tyrosine phosphatase-1B plays an important role in the negative signalling pathway of insulin. CoMSIA studies are performed on 1,2-naphthoquinone derivatives and different CoMSIA models were built to get the best related field.

A comparison between two polarizability parameters in chemical-biological interactions.

R.P. Verma* [Pomona Coll] and C. Hansch

Bioorg. Med. Chem. **13**, 2355-2372 (2005)

The use of two polarizability parameters NVE (sum of the valence electrons) and CMR (calculated molar refractivity) is compared in the formulation of QSAR for chemical-biological interactions was discussed.

Anti-inflammatory activity and QSAR studies of compounds isolated from Hyacinthaceae species and *Tachadenus longiflorus* Griseb.

K. du Toit, E.E. Elgorashi, S.F. Malan, S.E. Drewes, J. van Staden, N.R. Crouch and D.A. Mulholland* [U KwaZulu-Natal]

Bioorg. Med. Chem. **13**, 2561-2568 (2005)

Physicochemical descriptors like strain energy, enthalpy, dipole moment, log P, polarizability and molar refractivity were used in QSAR. This study produced three equations with significant prediction values for the anti-inflammatory activity and also provided valuable parameter guidelines for those properties influencing the anti-inflammatory activity of the studied compounds.

CoMFA, HQSAR and molecular docking studies of butitaxel analogues with β -tubulin.

S.L. Cunningham* [U Pittsburgh], B.W. Day and A.R. Cunningham
J. Mol. Mod. **11**, 48-54 (2005)

A series of 20 butitaxel analogues, paclitaxel and docetaxel were used to build 2-D and 3-D QSAR models were developed to investigate the properties associated with microtubule assembly and stabilization. Steric and electrostatic fields were used to built CoMFA with r^2 of 0.943 and q^2 of 0.376. HQSAR modeling of these same data generated an r^2 of 0.919 and a q^2 of 0.471.

Quantitative structure-activity relationships of mutagenic activity from quantum topological descriptors: triazenes and halogenated hydroxyfuranones (mutagen-X) derivatives.

P.L.A. Popelier* [U Manchester], P.J. Smith, and U.A. Chaudry

J. Comput.-Aid. Molec. Design **18**, 709-718 (2004)

3D-QSAR based on QM-derived descriptors at the B3LYP/6-311+(2d,p) level, yields a model with 3 variables, $r^2=0.859$ and $q^2=0.741$ for the mutagenicity of 23 triazenes; and at the HF/6-31G* level with 3 variables, $r^2=0.832$ and $q^2=0.720$ for 24 MX derivatives. Resolutions for existing mechanistic ambiguities are suggested and discussed.

 Quantitative Structure-Activity Relationships (cont'd)

Theoretical prediction of the Abraham hydrogen bond acidity and basicity factors from a reaction field method.

I. Cacelli* [U Pisa], S. Campanile, A. Giolitti, and D. Molin
J. Chem. Inf. Model. **45**, 327-333 (2005)

Atomic charges derived from quantum chemical calculations with inclusion of a solvent PCM model are shown to allow prediction of Abraham descriptors with a correlation coefficient of >0.97 , and thus are useful in predicting oral bioavailability. These descriptors may be useful for generating other QSAR relationships.

Structure based activity prediction of HIV-1 reverse transcriptase inhibitors.

M.R. de Jonge* [Janssen], L.M.H. Koymans, H.M. Vinkers, F.F.D. Daeyaert, J. Heeres, P.J. Lewi, and P.A.J. Janssen

J. Med. Chem. **48**, 2176-2183 (2005)

Up to 1000 low energy conformations of inhibitors are docked into HIV-1 RT and then the complex is energy minimized. Interaction energies to residues adjacent to the binding site are used to generate a linear fit to known binding affinities, resulting in a model with q^2 of 0.681.

Carbon Nanoparticles

Comparative analysis of surface electrostatic potentials of carbon, boron/nitrogen and carbon/boron/nitrogen model nanotubes.

P. Politzer* [U New Orleans], P. Lane, J.S. Murray, and M.C. Concha

J. Mol. Mod. **11**, 1-7 (2005)

B_xN_x and $C_{2x}B_xN_x$ model nanotubes were considered to study the electrostatic potentials on the inner and outer surfaces of a group of carbon. The inner surfaces are more positive than the corresponding outer ones and the outsides of B_xN_x tubes have characteristic patterns of alternating positive and negative regions, while the insides are strongly positive.

Molecular dynamics of transient oil flows in nanopores. II. Density profiles and molecular structure for decane in carbon nanotubes.

S. Supple* [Imperial College London] and N. Quirke

J. Chem. Phys. **122**, 10470601-10470608 (2005)

Narrow carbon nanotubes imbibe decane faster than broader tubes, with rates above 800 m/s. Diffusion is well-described with advection-diffusion equations in terms of friction and surface interactions. The variations of molecular structure with tube diameter and radial position in the tube are also presented.

1.2. *Biopolymers*

Bioinformatics

Comparison of substructural epitopes in enzyme active sites using self-organizing maps.

K. Kupas, A. Ultsch* [Marburg], and G. Klebe

J. Comput.-Aid. Molec. Design **18**, 697-708 (2004)

Clustering by emergent self-organizing maps of local regions described by tetrahedrons of pseudocenters in 72 binding cavities reproduces several of the 12 EC enzyme classifications considered, and sheds light on possible partners to orphan binding sites. Possible efficient application in large-scale comparisons cavity is discussed.



 Bioinformatics (cont'd)

Assigning new GO annotations to protein data bank sequences by combining structure and sequence homology.

J.V. Ponomarenko* [UCSD], P.E. Bourne, and I.N. Shindyalov

Proteins 58, 855-865 (2005)

A method for automated 'Gene Ontology' annotation of PDB entries and a comparison with (existing) SCOP annotations is presented. The combination of structure- and sequence-homology is vital for accuracy of new, derived annotations.

Amino acid coupling patterns in thermophilic proteins.

H.K. Liang, C.M. Huang, M.T. Ko* [Acad Sinica NanKang], and J.K. Hwang* [Nat'l Chiao Tung U]

Proteins 59, 58-63 (2005)

Statistical comparison of 'xdy' x-y residue-pair sequence patterns at *d* distance between meso- and thermophiles (74, resp. 15 genomes), reveals several highly significant patterns but no single dominant pattern. The absence of correlation with overall genomic GC content is confirmed.

A novel strategy for the identification of toxinlike structures in spider venom.

S. Kozlov* [Russian Acad Sci], A. Malyavka, B. McCutchen, A. Lu, E. Schepers, R. Herrmann, and E. Grishin

Proteins 59, 131-140 (2005)

An elegant combination of cDNA EST library construction of *A. orientalis* and database analysis reveals three distinct sequence motifs for spider toxins. Implications for evolutionary analysis, and for analysis of venoms from other genii are discussed.

The Protein Coil Library: A structural database of nonhelix, nonstrand fragments derived from the PDB.

N.C. Fitzkee, P.J. Fleming, and G.D. Rose* [J Hopkins U]

Proteins 58, 852-854 (2005)

The development of a non- α/β -structure library containing ~780,000 fragments from ~25,000 PDB entries, and user interface with query forms and interfaces to other databases, is described.

Protein domain of unknown function DUF1023 is an alpha/beta hydrolase.

M. Zheng, K. Ginalski* [U Texas], L. Rychlewski, and N.V. Grishin

Proteins 59, 1-6 (2005)

The as yet uncharacterized DUF1023 pfam-family is hypothesized as being an α/β -hydrolase with a Ser-His-Asp catalytic triad, based on sequence analysis and alignments, and secondary structure and fold predictions for all DUF1023 sequences. Analysis of their genomic context suggest a possible lipase activity.

Protein Sequence Analysis and Alignment

Protein classification based on text document classification techniques.

B.Y. Cheng, J.G. Carbonell, and J. Klein-Seetharaman* [U Pittsburgh]

Proteins 58, 955-970 (2005)

A decision tree and naive Bayes classification method based on *n*-gram counts is applied to GPCR's and shown to outperform previous SVM methods, at an accuracy of 93% and almost half residual error, and performs comparable to a search in PFAM. Accuracies for the nuclear receptor superfamily are around 95%.

Protein Sequence Analysis and Alignment (cont'd)

A new method for identification of protein (sub)families in a set of proteins based on hydrophathy distribution in proteins.

J. Panek* [U Queensland], I. Eidhammer, and R. Aasland

Proteins **58**, 923-934 (2005)

A method based on PCA and clustering in 'generalized hydrophathy' space, describing hydrophylic, hydrophobic or ambiguous residues in sequence segments, shows a reasonable separation of protein families of membrane proteins, cathepsins and anaerobic NAD biosynthesis. Limitations and possible improvements of the method are discussed.

Prediction of distant residue contacts with the use of evolutionary information.

S. Vicatos, B.V. Reddy, and Y. Kaznessis* [U Minnesota]

Proteins **58**, 935-949 (2005)

Identification of correlated mutations based on residue physicochemical properties, in stead of substitution matrices, is shown to give promising results, with an average accuracy of 27% (6-fold better than random) at 0.65 correlation for 127 families, and results vary widely between families.

Protein Structure Prediction

Protein complexes: structure prediction challenges for the 21st century.

P. Aloy, M. Pichaud, and R.B. Russell* [EMBL]

Curr. Opi. Stru. Biol. **15**, 15-22 (2005)

The availability of more sequence and structural data, faster computers, algorithms and concepts provide structural models with reasonable accuracy for a large fraction of the proteins present in an organism. These are useful to understand the molecular details of particular molecules or those seeking to design new drugs. The structure prediction involves simply finding the best homologous protein of known structure on which to construct a model.

A multibody, whole-residue potential for protein structures, with testing by Monte Carlo simulated annealing.

S. Mayewski* [Max Planck]

Proteins **59**, 152-169 (2005)

A data-base derived multi-body residue interaction potential on 'local environment signatures' is developed and can predict in a MC-SA setup the structure of 5 small proteins (20-38 residues) to 2.3-3 [AA] RMSD from the NMR structure. Improvements of the potential derivation, database analysis and conformational search method are discussed.

Comparative or Homology Modeling

Molecular dynamics simulations of the human CAR ligand-binding domain: deciphering the molecular basis for constitutive activity.

B. Windshügel* [Martin-Luther U], J. Jyrkkärinne, A. Poso, P. Honkakoski and W. Sippl
J. Mol. Mod. **11**, 69-79 (2005)

Homology models were used to investigate the basal activity of CAR and the effect of coactivator binding. The basal activity of CAR is explained by specific van-der-Waals interactions between amino acids on the LBD and its C-terminal activation domain (AF-2). GOLD program is used for docking and the interaction modes of structurally diverse agonists, giving insight into mechanisms by which ligands enhance CAR activity.



 Comparative or Homology Modeling (cont'd)

!

Progress and challenges in high-resolution refinement of protein structure models.

K.M. Misura and D. Baker* [U Washington]

Proteins **59**, 15-29 (2005)

A critical evaluation of a state-of-the-art refinement method in homology modeling. The forcefield used is able to discriminate unfolded, near-native and native states and could be used for precise refinement as well as rotamer searches in most cases of a test set of 10 proteins. Conformational sampling in the (near-native) condensed states is a confounding bottleneck. Other bottlenecks and possible solutions are discussed.

Analysis of GTPases carrying hydrophobic amino acid substitutions in lieu of the catalytic glutamine: Implications for GTP hydrolysis.

R. Mishra, S.K. Gara, S. Mishra, and B. Prakash* [Indian Inst Tech]

Proteins **59**, 332-338 (2005)

Homology models of ten non-oncogenic GTPase active Ras mutants show a solution to the paradox of activity without the catalytic Gln, whose role can be taken over by residues from inserts. Structural and mechanistic implications for GTPases in general are discussed.

Peptide Conformational Analysis

Competition between intramolecular hydrogen bonds and solvation in phosphorylated peptides: Simulations with explicit and implicit solvent.

S.E. Wong, K. Bernacki, and M. Jacobson* [UCSF]

J. Phys. Chem. B **109**, 5249-5258 (2005)

MD simulations investigate phosphorylated peptides. GB methods tend to over-estimate hydrogen bonding, however both these methods and explicit solvent provide a reasonable representation.

Protein Structure Analysis

A

Analysis of the interactions of ribonuclease inhibitor with kanamycin.Z. Wang, L. Zhang, J. Lu* [Peking U] and L. Zhang
J. Mol. Mod. **11**, 80-86 (2005)

Affinity module of Insight II molecular modeling program is used to determine relevant surface characteristics determining the interaction behavior. The electrostatic interactions and H-bond forces are the major factors for the molecular interaction between kanamycin and RI.

Global mapping of the protein structure space and application in structure-based inference of protein function.

J. Hou, S.-R. Jun, C. Zhang and S.-H. Kim* [UCB]

PNAS **102**, 3651-3656 (2005)

A map of the protein structure space was constructed by using the pairwise structural similarity scores calculated for all nonredundant protein structures. Proteins sharing similar molecular functions were found to colocalize in the protein structure space map. This scheme consistently outperformed other predictions made by using either the raw scores or normalized Z-scores of pairwise DALI structure alignment.

Protein Structure Analysis (cont'd)

Geometric preferences of crosslinked protein-derived cofactors reveal a high propensity for near-sequence pairs.

M.D. Swain and D.E. Benson* [Wayne State U]

Proteins **59**, 64-71 (2005)

A search in 500 proteins for mutations prone to CPDC by 'outer shell oxidation' reveals geometrical patterns similar to those of sulfur-bridges. From non-bonded contacts reported by PROCHECK from the PDB, 323 proteins with 'pre-attack' geometries, of which 55 local in sequence, were identified.

Properties of polyproline II, a secondary structure element implicated in protein-protein interactions.

M.V. Cubellis* [U Napoli], F. Cailleze, T.L. Blundell, and S.C. Lovell

Proteins **58**, 880-892 (2005)

A statistical analysis of occurrence and properties of PPII helices in the PDB is presented. They are evolutionarily conserved and on average contain 40% proline but can be proline-free as well, and Gly and Tyr are disfavored. They are entropically favored and implicated in unfolded states, amyloid formation and nucleic acid binding.

Flexibility of metal binding sites in proteins on a database scale.

M. Babor, H.M. Greenblatt, M. Edelman, and V. Sobolev* [Weizmann]

Proteins **59**, 221-230 (2005)

A large scale and thorough structural analysis of apo- and holo-structures of 210 metal-binding proteins shows that 40% undergo conformational rearrangements, in 14% involving the backbone, and in most only modest rearrangement of 1 or 2 sidechains is seen. Implications for metal-binding prediction methods are discussed.

Comparative structural analysis of TonB-dependent outer membrane transporters: Implications for the transport cycle.

D.P. Chimento, R.J. Kadner, and M.C. Wiener* [U Virginia]

Proteins **59**, 240-251 (2005)

Detailed analysis of substrate-bound and unbound structures of four transport channels reveals a hydrated, wide-gapped interface between the outer barrel and the inner hatch domain, comparable to known transient protein-protein interfaces. Implications for functional motion and energetics are discussed.

Evolutionarily conserved functional mechanics across pepsin-like and retroviral proteases.

M. Cascella, C. Micheletti, U. Rothlisberger, and P. Carloni* [SISSA]

J. Amer. Chem. Soc. **127**, 3734-3742 (2005)

Sequence alignment, classical MD on b-secretase, and estimates of the reaction free energies of different substrate/enzyme conformations together allow development of a simple topology-based energy functional that allows generalization of the functional motions across the aspartic proteases.

SH2 binding bite comparison: A new application of the SURFCOMP method.

C. Hofbauer and A. Aszodi* [Novartis]

J. Chem. Inf. Model. **45**, 414-421 (2005)

Comparison of the static binding site surfaces of Sap and Eat-2 SH2 domains using SURFCOMP suggests differences that might be exploited to gain selectivity in ligand design.

T

Protein Folding

Folding and binding: An extended family business.

G. Schreiber* [Weizmann Inst Sci] and L. Serrano

Curr. Opi. Stru. Biol. **15**, 1-3 (2005)

The Schreiber research group investigated from theoretical calculations and protein design to the analysis of the biological consequences of induced perturbations on systems biology *in vivo*. Luis' research group focused on the development of computational approaches to understand biological systems ranging from proteins to protein networks.

Natively unfolded proteins.

A.L. Fink* [U Calif]

Curr. Opi. Stru. Biol. **15**, 35-41 (2005)

New algorithms were developed to identify disordered regions of proteins and demonstrated their presence in cancer-associated proteins and proteins regulated by phosphorylation.

!

One gene, two diseases and three conformations: Molecular dynamics simulations of mutants of human prion protein at room temperature and elevated temperatures.

M.S. Shamsir and A.R. Dalby* [U Exeter]

Proteins **59**, 275-290 (2005)

Multiple MD simulations each of four forms of the prion, i.e. wild-type, the D178N pathological mutant, both with either of the 129(M,V) polymorphism, and at 300 and 500K, show decreased stability for the mutant, with higher stability in the 129M variants while the 129V leads to increased β -sheet formation. Conformations and transitions are analysed in detail.

Thermal unfolding simulations of a multimeric protein-Transition state and unfolding pathways.

J. Duan and L. Nilsson* [Karolinska Inst]

Proteins **59**, 170-182 (2005)

Detailed analysis of extensive unfolding simulations of a tetrameric protein, p53tet, reveals heterogeneous unfolding events, a relatively strong coupling between tetramerization and folding, and a hydrophobic driving force.

Folding time distributions as an approach to protein folding kinetics.

S. F. Chekmarev* [Inst Thermophysics], S. B. Krivov, and M. Karplus* [Harvard U]

J. Phys. Chem. B **109**, 5312-5330 (2005)

MD dynamics on a cubic lattice explore a 27-residue heteropolymer over a range of temperatures. The results suggest that care should be levied when folding data is interpreted in terms of the underlying kinetics.

Folding thermodynamics of peptides.

A. Irbäck* [Lund U] and S. Mohanty

Biophys. J. **88**, 1560-1569 (2005)

A simplified, solvent-free force field for ~20-mer peptide folding shows appropriate sequence dependence, although some sequences (Betanova) do not fold as uniformly as others (GB1m2 and GB1m3).

Protein Design and Engineering

Use of molecular dynamics in the design and structure determination of a photoinducible β -hairpin.

V. Krautler, A. Aemissegger, P. H. Hunenberger, D. Hilvert, T. Hansson, and W. F. van Gunsteren* [ETH]

J. Amer. Chem. Soc. **127**, 4935-4942 (2005)

Classical explicit solvent MD simulations (in water and ethanol) are able to predict the ensemble of structures of a set of designed β -hairpins consistent with experiment. The paper includes the theory and NMR experiment on the set of peptides containing a series of photoswitchable diazobenzene linkers a different lengths and configuration.

Tryptophan side chain electrostatic interactions determine edge-to-face vs. parallel-displaced tryptophan side chain geometries in the designed β -hairpin "trpzip2."

O. Guvench, and C. L. Brooks III* [Scripps]

J. Amer. Chem. Soc. **127**, 4668-4674 (2005)

The geometries (and free energetics) of the interaction of four tryptophan residues in the 12-residue designed β -hairpin tripzip2 are investigated with MD simulation in explicit solvent. The results highlight the importance of the electrostatic multipole moments to stability the edge-to-face interactions of two pairs of exposed tryptophans.

Protein Hydration

A "solvated rotamer" approach to modeling water-mediated hydrogen bonds at protein-protein interfaces.

L. Jiang, B. Kuhlman, T. Kortemme, and D. Baker* [U Washington]

Proteins **58**, 893-904 (2005)

A model for the inclusion of explicit water molecules as extended rotamer-states of residues at protein-protein interfaces, and based on analysis of water molecules in high-resolution X-ray structures, is presented and used to predict the location of water molecules and to improve the accuracy of sidechain-identity prediction at interfaces. Significant advantages and improvements with respect to continuum solvent models, and ways for further improvement of the model, are discussed.

Hydrophobic tendency of polar group hydration as a major force in type I antifreeze protein recognition.

C. Yang and K.A. Sharp* [U Pennsylvania]

Proteins **59**, 266-274 (2005)

MD simulations (1ns) of wild-type and anti-freeze-active mutants of type 1 THP show water structure around polar groups in the ice-binding region similar to that around hydrophobic solutes, while an anti-freeze inactive mutant shows 'normal' hydrophylic water structure.

Sensitivity of polar solvation dynamics to the secondary structures of aqueous proteins and the role of surface exposure of the probe.

S. Bandyopadhyay* [IIT], S. Chakraborty, S. Balasubramanian, and B. Bagchi* [IIS]

J. Amer. Chem. Soc. **127**, 4071-4075 (2005)

Time correlation functions for water around various regions of the villin headpiece subdomain protein are explored from previous MD trajectories generated by this group. The results suggest that the more surface exposed a probe is (such as either an internal or associated fluorescent molecule), the faster the solvation dynamics are.

Protein Electrostatics and Titration

Statistical criteria for the identification of protein active sites using theoretical microscopic titration curves.

J. Ko, L.F. Murga, P. Andre, H. Yang, M.J. Ondrechen* [N-E U], R.J. Williams, A. Agunwamba, and D.E. Budil

Proteins **59**, 183-195 (2005)

A method for automated selection of nonsigmoidal behavior of computed titration curves is shown to significantly improve and speed up the identification of possibly functionally relevant clusters of residues with such behavior in 40 out of 44 protein structures. Four successful cases are discussed in detail.

Protein Dynamics

A systems biology perspective on protein structural dynamics and signal transduction.

F. Rousseau* [Vrije U Brussel] and J. Schymkowitz

Curr. Opin. Stru. Biol. **15**, 23-30 (2005)

In silico methods are developed to identify networks of cooperative residues in proteins and applied to analyze the important classes of modular signal transduction domains.

Molecular dynamics simulation of entropy driven ligand escape process in heme pocket.

S.-Y. Sheu* [Nat'l Yang-Ming U]

J. Chem. Phys. **122**, 10490501-10490507 (2005)

Ligand motions in a spherical cavity entropically favor the surface and are then gated by protein structure fluctuations.

How similar are protein folding and protein binding nuclei? Examination of vibrational motions of energy hot spots and conserved residues.

T. Haliloglu* [Bogazici U], O. Keskin, B. Ma, and R. Nussinov* [NCI Frederick]

Biophys. J. **88**, 1552-1559 (2005)

Binding and folding (self-binding) contacts generally vibrate at high frequencies compared to the rest of a protein.

Relaxation kinetics and the glassiness of native proteins: Coupling of timescales.

C. Baysal* [Sabanci U] and A.R. Atilgan

Biophys. J. **88**, 1570-1576 (2005)

Analyses of BPTI dynamics from MD simulations indicate that proteins are functional when the temperature is such that motions on three time scales come into play, slow for motions along the folded state envelope, fast for diversions into pockets off of the folded state envelope, and intermediate for hops between the pockets.

Open interface and large quaternary structure movements in 3D domain swapped proteins: Insights from molecular dynamics simulations of the C-terminal swapped dimer of ribonuclease A.

A. Merlino, M.A. Ceruso, L. Vitagliano, and L. Mazzarella* [Complesso U Monte Sant'Angelo]

Biophys. J. **88**, 2003-2012 (2005)

Domain-swapping often results in high flexible dimers, as exemplified with RNase, where simulations of the C-dimer (in which the domains at the C-terminus are swapped) indicate that its increased flexibility over the N-dimer occurs without loss of native fold or dynamics of the functionally active site. Perhaps the flexibility change is related to pathological aggregation in some cases.

Ligand Binding

Prediction of binding modes for ligands in the cytochromes P450 and other heme-containing proteins.

S.B. Kirton, C.W. Murray* [Astex], M.L. Verdonk, and R.D. Taylor

Proteins **58**, 836-844 (2005)

The performance of the ChemScore scoring function within the Gold docking program is shown to significantly outperform the GoldScore scoring function for binding mode prediction of ligands in heme-proteins, and for most failures scoring function, and not the search algorithm, is the likely problem. An improved version of ChemScore and more suggestions for improvement are presented.

Comparative analysis of protein-bound ligand conformations with respect to Catalyst's conformational space subsampling algorithms.

J. Kirchmair, C. Laggner, G. Wolber, and T. Langer* [U Innsbruck]

J. Chem. Inf. Model. **45**, 422-430 (2005)

Ligands from a set of 510 co-crystal structures were run through Catalyst's conformational model generation algorithm and compared to the observed conformation. A fitting of at least one conformer with an RMS value of <1.50Å was found in over 80% of cases, although bioactive conformers have higher computed energies than the global computed minimum.

A

Searching for a reliable orientation of ligands in their binding site: Comparison between a structure-based (Glide) and a ligand-based (FIGO) approach in the case study of PDE4 inhibitors.

P. Gratteri* [U Florence], C. Bonaccini, and F. Melani

J. Med. Chem. **48**, 1657-1665 (2005)

A method called FIGO, which overlays compounds based on their Grid-generated molecular interaction fields, is applied to PDE4. The results are compared to those from structure-based docking.

Molecular dynamics simulation of cocaine binding with human butyrylcholinesterase and its mutants.

A. Hamza, H. Cho, H.-H. Tai, and C.-G. Zhan* [U Ky]

J. Phys. Chem. B **109**, 4776-4782 (2005)

MD simulations of the enzyme BChE (and point mutants) interacting with cocaine, based on the recent crystal structure, confirm interpretations made in earlier simulations of homology models despite significant differences at the acyl binding site.

Enzyme Catalysis

A theoretical DFT investigation of the lysozyme mechanism: Computational evidence for a covalent intermediate pathway.

A. Bottoni* [U Bologna], G.P. Miscione* [U Bologna], and M. De Vivo

Proteins **59**, 118-130 (2005)

B3LYP calculations on the lysozyme catalytic center consisting of β -methylglucoside, Asp52, Glu35 and a water, along three possible mechanisms with 10 intermediate states in total support a covalent intermediate, and not an 'oxocarbenium anion'-type pathway.

Enzyme Catalysis (cont'd)

Molecular dynamics simulations of human butyrylcholinesterase.

D. Suarez* [U Oviedo] and M.J. Field

Proteins **59**, 104-117 (2005)

A detailed analysis of dynamics, structure and several key events of BuChE from several 5-10 ns MD runs is presented, most notably ion mobility, water-structure and -bridges in the protein interior. Implications for substrate binding and a comparison with a similar analysis of AChE are discussed.

Mechanisms of antibiotic resistance: QM/MM modeling of the acylation reaction of a class A β -lactamase with benzylpenicillin.

J. C. Hermann, C. Hensen, L. Ridder, A. J. Mulholland* [U Bristol], and H.-D. Holtje* [U Dusseldorf]

J. Amer. Chem. Soc. **127**, 4454-4465 (2005)

QM/MM simulations at the AM1 level (corrected by DFT calculations) are performed on models of β -lactamase with a bound benzylpenicillin molecule. Using a decomposition analysis it is shown that the oxyanion hole is important for stabilizing the transition state along with demonstrated key interactions of charged residues (in addition to Asn132) in the active site.

Theoretical study of the truncated hemoglobin HbN: Exploring the molecular basis of the NO detoxification mechanism.

A. Crespo, M. A. Marti, S. G. Kalko, A. Morreale, M. Orozco, J. L. Gelpi, F. Javier Luque* [U Barcelona], and D. A. Estrin* [U Buenos Aires]

J. Amer. Chem. Soc. **127**, 4433-4444 (2005)

QM/MM simulations (at the DFT level using SIESTA) along with classical MD simulations probe the protein dynamics, O₂ affinity and NO reaction with O₂ on the heme of oxy-truncated hemoglobin N (which is the protein thought responsible for tuberculosis resistance to NO).

Dynamical flexibility and proton transfer in the arginase active site probed by ab initio molecular dynamics.

I. Ivanov* [U Penn] and M.L. Klein

J. Amer. Chem. Soc. **127**, 4010-4020 (2005)

Car-Parrinello extended Lagrangian ab initio MD simulations (on the ~10 ps time scale) are applied to a minimal (periodic and solvated) model of the active site of arginase. The calculations were sufficient to observe the proton (deuterium) transfer.

Macrophomate synthase: QM/MM simulations address the Diels-Alder versus Michael-Aldol reaction mechanism.

C.R.W. Guimaraes, M. Udier-Blagovic, and W.L. Jorgensen* [Yale U]

J. Amer. Chem. Soc. **127**, 3577-3588 (2005)

Introducing a new link atom approach at the QM/MM interface, QM/MM simulations with MC and FEP simulation probe the Diels-Alder reaction catalyzed by the enzyme macrophomate synthase.

Computational investigation of irreversible inactivation of the zinc-dependent protease carboxypeptidase A.

J. B. Cross, T. Vreven, S. O. Meroueh, S. Mobashery, and H. B. Schlegel* [Wayne State U]

J. Phys. Chem. B **109**, 4761-4769 (2005)

ONIOM QM/MM calculations, with ab initio HF, AM1 and AMBER parm99 empirical force field levels probe the mechanism-based inhibition mediated by zinc in zinc proteases.

Enzyme Catalysis (cont'd)

Relative contributions of desolvation, inter- and intramolecular interactions to binding affinity in protein kinase systems.

P.A. Sims, C.F. Wong* [U Missouri], D. Vuga, J.A. McCammon, and B.M. Sefton

J. Comput. Chem. **26**, 668-621 (2005)

Water plays an important role in ligand binding according to decompositions of sensitivity analyses based on the Poisson continuum model. Ligand-protein electrostatic interactions are able to overcome the desolvation penalty for a large ligand, found in PKA-PKI, but not (or barely) for the small ligands found in CDK2-deschloroflavopiridol or LCK-PP2

Protein-Protein Interactions

New methodologies for measuring protein interactions *in vivo* and *in vitro*.

J. Piehler* [Johann Wolfgang Goethe U]

Curr. Opi. Stru. Biol. **15**, 4 -14 (2005)

Generic methods are established for monitoring protein interactions *in vivo* by protein fragment complementation and for screening protein interactions *in vitro* by highly parallel solid-phase techniques. The study of protein interactions on the single-molecule level has become an important tool for understanding protein function *in vivo* and *in vitro*.

Cation- π interactions in protein-protein interfaces.

P.B. Crowley* [U Nova Lisboa] and A. Golovin

Proteins **59**, 231-239 (2005)

Cation- π interactions were identified in nearly half of all protein interfaces studied, and dominated by Arg-Tyr pairs. Structural, energetical and statistical features of these interactions are discussed in detail. Possible implications for protein-protein interaction prediction are discussed.

Membrane Proteins and Lipid-Peptide Interactions

Proton binding within a membrane protein by a protonated water cluster.

F. Garczarek, L.S. Brown, J.K. Lanyi, and K. Gerwert* [Ruhr-U Bochum]

PNAS **102**, 3633 -3638 (2005)

The influence of several mutations on the proton release network and the continuum change were investigated. A protonated water cluster consisting in total of one proton and about five water molecules surrounded by six side chains and three backbone groups are identified. The observed perturbation of proton release by many single-residue mutations is explained by the influence of numerous side chains on the protonated H bonded network.

Understanding the energetics of helical peptide orientation in membranes.

D. Sengupta, L. Meinhold, D. Langosch, G.M. Ullmann* [U Heidelberg], and J.C. Smith* [U Heidelberg]

Proteins **58**, 913-922 (2005)

A method combining an atomic description of the peptide, a solvent-headgroup-core 5-slab continuum dielectric model, electrostatic solvation, and surface-area dependent solvent cavity formation, is shown to accurately predict helix tilt angles for 19-, 25- and 30-mer 'WALP' peptides, melittin and glycophorin monomer.



 Membrane Proteins and Lipid-Peptide Interactions (cont'd)

!

Properties of integral membrane protein structures: Derivation of an implicit membrane potential.

M.B. Ulmschneider* [U Rome Sapienza], M.S. Sansom, and A. Di Nola

Proteins **59**, 252-265 (2005)

The distributions of residues in the membrane region of all known $<4\text{\AA}$ α -helical membrane proteins, shows these to be much more hydrophobic than the protein interior, and a preference for Arg (and less for Lys) at the inner leaflet. A derived potential of mean force could be used to correctly orient 9 membrane proteins, and 4 α -helices inserted as well as interfacial.

Role of cholesterol and polyunsaturated chains in lipid-protein interactions: Molecular dynamics simulation of rhodopsin in a realistic membrane environment.

M.C. Pitman, A. Grossfield, F. Suits, and S.E. Feller* [Wabash U]

J. Amer. Chem. Soc. **127**, 4576-4577 (2005)

MD simulations investigate rhodopsin in a complex bilayer mixture of 24 cholesterol, 49 SDPC and 50 SDPE lipids. The protein appears to be preferentially solvated by the 22-carbon polyunsaturated chain; in the 100+ ns-length simulations, every lipid interacts with the protein at least once.

Permeation of particle through a four-helix-bundle model channel.

B. Xue* [Nanjing U], Y. Su, and W. Wang

J. Chem. Phys. **122**, 10470301-10470313 (2005)

The permeability of a coarse-grained four-helix bundle channel to ions depends on the temperature and inversely on the ion-channel attraction, according to nonequilibrium MD simulations. Permeation is observed for voltages above a certain threshold, and mean first passage time decreases with voltage.

Targeted molecular dynamics of an open-state KcsA channel.

M. Compain* [U Franche-Comté], F. Picaud, C. Ramseyer, and C. Girardet

J. Chem. Phys. **122**, 13470701-13470708 (2005)

The transition from the closed (PDB 1K4C, crystallographic) to the open (PDB 1JQ1, EPR-based) configuration of the bacterial potassium channel can be initiated by a minor force applied to the cytoplasmic end of the M2 helix by way of a zipper-like mechanism. Additional forces are needed to complete the opening, however, and an alternative open state is attained after removal of the constraints.

Molecular dynamics study of the lung surfactant peptide SP-B1-25 with DPPC monolayers: Insights into interactions and peptide position and orientation.

S.K. Kandasamy and R.G. Larson* [U Michigan]

Biophys. J. **88**, 1577-1592 (2005)

Simulation of the N-terminal 25-residue segment from lung surfactant protein with DPPC demonstrates that the helix is bound parallel to the interface, that the first 8 residues are important for anchoring, and that hydrogen bond donors from the peptide interact strongly with head group hydrogen bond receptors. Charged residues come into play.

Simulation studies of protein-induced bilayer deformations, and lipid-induced protein tilting, on a mesoscopic model for lipid bilayers with embedded proteins.

M. Venturoli, B. Smit, and M.M. Sperotto* [Tech U Denmark]

Biophys. J. **88**, 1778-1798 (2005)

Hydrophobic mismatch results in protein tilt (if the hydrophobic section on the protein is too long) and a single damped oscillation in lipid thickness (whether too long or too short), according to mesoscopic simulations with dissipative dynamics.

Membrane Proteins and Lipid-Peptide Interactions (cont'd)

Molecular packing and packing defects in helical membrane proteins.

P.W. Hildebrand* [U Med Berlin], K. Rother, A. Goede, R. Preissner, and C. Frömmel

Biophys. J. **88**, 1970-1977 (2005)

Membrane protein structural analysis using a Voronoi procedure indicates that membrane proteins are loosely packed, especially near active sites, which are lined with polar residues if they are to transport ions or nonpolar residues if they are in hinge regions for molecular reorganizations.

Protein-Nucleic Acid Interactions

Conformational transition pathway of polymerase β /DNA upon binding correct incoming substrate.

K. Arora and T. Schlick* [NYU]

J. Phys. Chem. B **109**, 5358-5367 (2005)

A stochastic difference equation methods that approximates long-time dynamics is applied to simulate the pol β active site changes upon binding of the substrate.

Nucleic Acids

Structure, recognition properties, and flexibility of the DNA-RNA hybrid.

A. Noy, A. Perez, M. Marquez, F. Javier Luque* [U Barcelona], and M. Orozco* [U Barcelona]

J. Amer. Chem. Soc. **127**, 4910-4920 (2005)

MD simulation is applied to understand the structure, dynamics and hydration properties of DNA-RNA hybrids.

Effect of PNA backbone modifications on cyanine dye binding to PNA-DNA duplexes investigated by optical spectroscopy and molecular dynamics simulations.

I. Dilek, M. Madrid, R. Singh, C. P. Urrea, and B. A. Armitage* [CMU]

J. Amer. Chem. Soc. **127**, 3339-3345 (2005)

MD simulation is used to supplement indirect structural data from experiment to better understand the interaction of a dye in the minor groove of a DNA-PNA duplex where the PNA is backbone is modified.

The stretched intermediate model of B-Z DNA transition.

W. Lim* [Natl U Singapore] and Y.P. Feng

Biophys. J. **88**, 1593-1607 (2005)

Does the B-Z transition follow the Harvey mechanism, which should be hampered by a steric conflict, or by way of an overstretched intermediate? A natural path for base reorientation from an unwound, overstretched intermediate is observed, based on simulations done using the stochastic difference equation method. An experiment is proposed that would identify the stretched intermediate state.

Molecular dynamics simulations of duplex stretching reveal the importance of entropy in determining the biomechanical properties of DNA.

S.A. Harris, Z.A. Sands, and C.A. Laughton* [U Nottingham]

Biophys. J. **88**, 1684-1691 (2005)

The role of entropy in producing elasticity of biological material is highlighted in this simulation of DNA stretching, which uses on a combination of atomistic modeling and statistical physics to successfully reproduce experiments.

Lipids and Surfactants

An ab initio study on the torsional surface of alkanes and its effect on molecular simulations of alkanes and a DPPC bilayer.

J. B. Klauda, B. R. Brooks, A. D. MacKerell, Jr., R. M. Venable, and R. W. Pastor* [FDA]

J. Phys. Chem. B **109**, 5300-5311 (2005)

A large series of normal alkane conformations are studied with high level QM to refine the CHARMM27 molecular mechanics force field.

Thermodynamics of the liquid states of Langmuir monolayers.

L. Villalobos* [U Puerto Rico Mayagüez], Y.M. López-Álvarez, B. Pastrana-Ríos, and G.E. López

J. Chem. Phys. **122**, 10470101-10470106 (2005)

A course-grained lipid simulation of the pressure-area curve in a Langmuir-Blodgett trough illustrates the coexistence of fluid-expanded and compressed phases. Distance and enthalpy distributions were computed to illustrate the coexistence region.

Concentration effects of volatile anesthetics on the properties of model membranes: A coarse-grain approach.

M. Pickholz* [U Pennsylvania, U Campinas], L. Saiz, and M.L. Klein

Biophys. J. **88**, 1524-1534 (2005)

Using one neutral site each for the 8-halothane and the 3-atom water molecules and 13 sites for the 118-atom DMPC molecules, the headgroups each consisting of an +e/78-charged choline site and a -e/78-charged phosphate site, large scale (512-lipid-molecule) bilayer simulations with 6 different high halothane concentrations showed that halothane would partition just inside or outside of the headgroups, increasing lipid spacing and decreasing lipid disorder near the headgroups.

2H-NMR study and molecular dynamics simulation of the location, alignment, and mobility of pyrene in POPC bilayers.

B. Hoff, Erik Strandberg, A.S. Ulrich, D.P. Tieleman, and C. Posten* [U Karlsruhe]

Biophys. J. **88**, 1818-1827 (2005)

Solid state NMR and MD simulations agree that, over a few ns, pyrene is oriented with its long axis within ~30° of parallel to the bilayer normal. MD positions the pyrene just below the lipid headgroups.

Carbohydrates

Computational study of the dynamics of mannose disaccharides free in solution and bound to the potent anti-HIV virucidal protein cyanovirin.

C. J. Margulis* [U Iowa]

J. Phys. Chem. B **109**, 3639-3647 (2005)

MD simulations with the OPLS-AA force field and an Ewald treatment look at the structure and dynamics of a sugar alone and interacting with cyanovirin. Two binding modes of the sugar are probed with the high affinity site preferring the solvent favored conformation.

1.3. Polymers

Prediction of lower critical solution temperature of *N*-isopropylacrylamide-acrylic acid copolymer by an artificial neural network model.

H. Kay* [Hacettepe U], S.A. Tuncel, A. Elkamel, and E. Alper
J. Mol. Mod. **11**, 55-60 (2005)

The LCST of *N*-isopropylacrylamide-acrylic acid copolymer as a function of chain-transfer agent/initiator mole ratio, acrylic acid content of copolymer, concentration, pH and ionic strength of aqueous copolymer solution was investigated. An artificial neural network model that is able to predict the lower critical solution temperature was developed. The predictions from this model compare well against both training and test data sets with an average error less than 2.53%.

Molecular dynamics simulations of polymer transport in nanocomposites.

T. Desai* [Rensselaer Polytech Inst], P. Koblinski, and S.K. Kumar

J. Chem. Phys. **122**, 13491001-13491008 (2005)

Within one radius of gyration of a nanosphere, polymer diffusivity is increased over bulk if the nanosphere surface is repulsive, and reduced if it is attractive. This is similar to polymer behavior near a flat surface. Diffusivity is also markedly reduced if only one monomer is pinned to the surface, emphasizing the importance of care with boundary conditions.

1.4. Surfaces, Catalysts, and Material Subjects

Molecular dynamics simulations of grafted polyelectrolytes on two opposing walls.

O.J. Hehmeyer* [Princeton U] and M.J. Stevens

J. Chem. Phys. **122**, 13490901-13490911 (2005)

When two surfaces are coated with either poly(styrene sulfonate) or double-stranded DNA (flexible and stiff respectively, both cases simulated with explicit counterions), their apposition results in mutual recoil of the molecular brushes to avoid interpenetration.

2. METHODOLOGY

Quantitative Structure-Activity Relations

A novel method of estimation of lipophilicity using distance-based topological indices: dominating role of equalized electronegativity.

V.K. Agrawal* [APS U], M. Gupta, J. Singh and P.V. Khadikar

Bioorg. Med. Chem. **13**, 2109-2120 (2005)

A new method is proposed to estimate lipophilicity of a heterogeneous set of 223 compounds based on the use of equalized electronegativity along with topological indices. An excellent results were obtained in multiparametric regression upon introduction of indicator parameters and are discussed critically on the basis various statistical parameters.

Conformational restrictions in ligand binding to the human intestinal di-/tripeptide transporter: implications for design of hPEPT1 targeted prodrugs.

J. Våbenø, C.U. Nielsen, B. Steffansen, T. Lejon, I. Sylte, F.S. Jørgensen and K. Luthman* [U Tromsø]

Bioorg. Med. Chem. **13**, 1977-1988 (2005)

A new computational method is developed to aid the design of dipeptidomimetic pro-moieties targeting the human intestinal di-/tripeptide transporter hPEPT1. An inverse linear relationship was obtained between ΔE_{bbone} and $\log 1/K_i$. The compounds are classified as high affinity ligands all have $\Delta E_{\text{bbone}} < 1$ kcal/mol, whereas medium and low-affinity compounds have ΔE_{bbone} values in the range 1-3 kcal/mol.

Conformational Search and Analysis

On the perception of molecules from 3D atomic coordinates.

P. Labute [Chem Computing Group]

J. Chem. Inf. Model. **45**, 215-221 (2005)

A maximum weighted matching graph algorithm is applied towards identifying hybridization states, bond orders, and formal charges in order to generate 3D chemical structures from 2D structures.

Potentials and Parameters

Inferring ideal amino acid interaction forms from statistical protein contact potentials.

P. Pokarowski* [Warsaw U], A. Kloczkowski, R.L. Jernigan, N.S. Kothari, M. Pokarowska, and A. Kolinski

Proteins **59**, 49-57 (2005)

A thorough analysis of 29 published residue contact potentials shows they fall in two classes, which are related to either of the two published by Miyazawa & Jernigan [Proteins 1999;34:49-68]. and can be interpreted as residue water-protein transfer energies and residue interaction energies in the protein, respectively. It is noted that the actual CPs have additional elements of specific value that are critical for their application.

The key role of atom types, reference states, and interaction cutoff radii in the knowledge-based method: New variational approach.

A.M. Ruvinsky* [Algodign] and A.V. Kozintsev

Proteins **58**, 845-851 (2005)

The strong dependence of appearance and reliability of derived "knowledge-based potentials" on choice of atom types and sub-types is investigated in detail, and the dependence and reliability of (re-)docking 130 complexes from the PDB with these potentials is shown, ranging from <20% within 2 AA for 6 atom types, to ~60% at the optimal 18 or 19 atom types.

Zn protein simulations including charge transfer and local polarization effects.

D.V. Sakharov, and C. Lim* [Acad Sinica]

J. Amer. Chem. Soc. **127**, 4921-4929 (2005)

In an attempt to improve the treatment of metal ions in protein simulation, a force field is developed that includes local polarization and charge transfer for zinc and compared to standard additive treatments. This potential adds to the standard Coulombic and vdw potential a local polarizability on Zn and charge transfer from directly attached Cys sulfur or His nitrogens.

Comparative study of generalized Born models: Born radii and peptide folding.

J. Zhu, E. Alexov, and B. Honig* [Columbia U]

J. Phys. Chem. B **109**, 3008-3022 (2005)

None of the GB models are perfect and each has different strengths ranging from closer agreement to PB (at a significant computational cost) to better sampling (with simpler GB models and a united atom force field). Although each method catches some essential elements of folding, deficiencies remain, and the transferability to other force fields (other than GROMOS96 force field) is questionable.

A multiscale coarse-graining method for biomolecular systems.

S. Izvekov and G. A. Voth* [U Utah]

J. Phys. Chem. B **109**, 2469-2473 (2005)

Using a force-matching procedure where atomic forces are propagated upward in scale with a time-averaged windowing, provides a means to develop realistic coarse-grained potentials. Application is demonstrated with a DPMC lipid bilayer.

 Potentials and Parameters (cont'd)

Empirical force-field assessment: The interplay between backbone torsions and noncovalent term scaling.

E.J. Sorin and V.S. Pande* [Stanford U]

J. Comput. Chem. **26**, 682-690 (2005)

The interplay between nonbonded interactions and torsion energies was found to affect ensemble average heliophilicity for poly-Ala peptides and varies significantly between force fields, according to distributed computing MD simulations.

Fluctuating charge normal modes: An algorithm for implementing molecular dynamics simulations with polarizable potentials.

L.R. Olano and S.W. Rick* [U New Orleans]

J. Comput. Chem. **26**, 699-707 (2005)

Compared to using fictitious masses for the fluctuating charges, it is more efficient to use a few (two) normal modes for the fluctuating charges in each molecule. This approach is tested with T4P-FQ water and compared to previous FQ approaches. In particular, it allows time steps of up to 1.5 fs and even 2.0 fs, whereas the usual method requires time steps of 1.0 fs.

Development of a force field for Li₂SiF₆.

A. Liivat, A. Aabloo, and J.O. Thomas* [Uppsala U]

J. Comput. Chem. **26**, 716-724 (2005)

Using QM and empirical facts and the crystal structure, parameters for MD simulations were obtained for dilithium silicon hexafluoride. The parameters were used to assess the space group of the crystal, leading to the conclusion that it is P321 rather than F₃m1.

An improved nucleic acid parameter set for the GROMOS force field.

T.A. Soares, P.H. Hünenberger, M.A. Kastenzholz, V. Kräutler, T. Lenz, R.D. Lins, C. Oostenbrink, and W.F. van Gunsteren* [Swiss Fed Inst Tech]

J. Comput. Chem. **26**, 725-737 (2005)

The 45A4 force field has been improved and now gives variations from expected structures on the order of their uncertainties.

A new force field for atomistic simulations of aqueous tertiary butanol solutions.

M.E. Lee* [Max-Planck-Inst] and N.F.A. van der Vegt

J. Chem. Phys. **122**, 11450901-11450913 (2005)

A force field for *tert* butanol solutions with simple point charge waters was developed and found to produce appropriate clustering for solutions of 2-98%. !

Solvation free energies of amino acid side chain analogs for common molecular mechanics water models.

M.R. Shirts* [Stanford U] and V.S. Pande

J. Chem. Phys. **122**, 13450801-13450813 (2005)

Using the dramatic improvements available with modern free energy techniques, the author's compared six standard water models with precisions of .02-.06 kcal/mol and found TIP3-MOD to be most accurate at predicting OPLS-AA side chain hydration energy. They also further tuned the TIP3 water model to produce zero average error with negligible effects on pure water behavior. !

Boundary Conditions

Constant-pressure and constant-surface tension simulations in dissipative particle dynamics.

A.F. Jakobsen* [U Southern Denmark]

J. Chem. Phys. **122**, 12490101-12490108 (2005)

A Langevin pressure piston is shown to provide faster equilibration and shorter correlation times than standard pressure pistons for constant pressure and constant surface tension simulations.

Solvation Energy

A coupled reference interaction site model/molecular dynamics study of the potential of mean force curve of the SN_2 Cl- + CH_3Cl reaction in water.

H. Freedman and T. N. Truong* [U Utah]

J. Phys. Chem. B **109**, 4726-4730 (2005)

MD simulations are analyzed with a RISM approach to estimate PMFs of a nucleophilic substitution reaction. This provides a cost effective methodology for looking at solution reactions.

Evaluation of Poisson solvation models using a hybrid explicit/implicit solvent method.

M. S. Lee* [USARID], and M. A. Olson

J. Phys. Chem. B **109**, 5223-5236 (2005)

A hybrid explicit/implicit solvent model is applied to evaluate implicit solvent models. The effect of different surfaces and probe radii are probed.

Molecular Dynamics

On the efficiency of exchange in parallel tempering Monte Carlo simulations.

C. Predescu* [UC Berkeley], M. Predescu, and C. V. Ciobanu

J. Phys. Chem. B **109**, 4189-4196 (2005)

Replica exchange and parallel tempering calculations are becoming very popular these days; this work investigates the efficiency of the exchange and proposes metrics that find the optimal switching probability (at 38.74%).

A simple method for faster nonbonded force evaluations.

M.-Y. Shen and K.F. Freed* [U Chicago]

J. Comput. Chem. **26**, 691-698 (2005)

A nearly 5-fold speedup for nonbond energies was achieved in TINKER by code improvements such as eliminating SQRTs and / from interatomic distance calculations and eliminating IF statements from loops.

From molecular dynamics to hydrodynamics: A novel Galilean invariant thermostat.

S.D. Stoyanov* [Unilever] and R.D. Groot

J. Chem. Phys. **122**, 11411201-11411208 (2005)

By combining two previously defined thermostats, one which produces high viscosity and one which produces low, the Nosé-Hoover-Lowe-Andersen thermostat uses central forces and allows tuning of the viscosity.

Molecular Dynamics (cont'd)

Methodological problems in pressure profile calculations for lipid bilayers.

J. Sonne* [Tech U Denmark], F.Y. Hansen, and G.H. Peters

J. Chem. Phys. **122**, 12490301-12490309 (2005)

!

New methods for evaluation of lateral pressure profiles in lipid bilayers, of great interest for understanding membrane protein partitioning and function, deal with the problem that they are not uniquely defined (because they depend on an arbitrary contour interval) and including Ewald electrostatics. Contour integrals leading to Irving-Kirkwood and Harasima versions of the local tensors give similar results with DPPC, and usage of Ewald electrostatics based on the Harasima tensor gives profiles similar to those obtained with long cutoffs.

Free Energy Methods

Absolute and relative entropies from computer simulation with applications to ligand binding.

J. Carlsson and J. Aqvist* [Uppsala U]

J. Phys. Chem. B **109**, 6448-6456 (2005)

Evaluation of the Schlitter and quasiharmonic methods for estimating entropies from a covariance matrix of atomic fluctuations from MD is presented. A new method for estimating rotational entropies based on variances in Euler angles is proposed.

Optimizing the driving function for nonequilibrium free-energy calculations in the linear regime: A variational approach.

M. de Koning* [U São Paulo]

J. Chem. Phys. **122**, 10410601-10410606 (2005)

The optimal time course for λ in slow growth TI simulations can be ascertained by some numerical sampling based on an analytical approach that minimizes entropy production. The fluctuation dissipation theorem in the linear response regime is used to assess entropy production, which is then minimized by solving the Euler-Lagrange equation.

Simulation of conformational transitions by the restricted perturbation-targeted molecular dynamics method.

A. van der Vaart* [Harvard U and U Louis Pasteur] and M. Karplus

J. Chem. Phys. **122**, 11490301-11490306 (2005)

In restricted perturbation MD, a single MD simulation with a method like targeted MD, but with limits on the conformational perturbation allowed, gives a more efficient, lower energy free energy profile. The method is illustrated using alanine dipeptide with analytical continuum electrostatics.

QM/MM

Computational methods for the study of enzymic reaction mechanisms III: A perturbation plus QM/MM approach for calculating relative free energies of protonation.

P.L. Cummins and J.E. Gready* [Australian National U]

J. Comput. Chem. **26**, 661-668 (2005)

!

The free energy of protonation of dihydrofolate-N and Asp27 in dihydrofolate reductase was computed using TI with perturbation of the semiempirical QM region. The results were similar to the linear response approximation results for some choices of the QM region, but differed in the components (i.e. QM and QM/MM).

 QM/MM (cont'd)

Computing kinetic isotope effects for chorimate mutase with high accuracy. A new DFT/MM strategy.

S. Marti, V. Moliner* [U Jaume], I. Tunon* [U Valencia], and I. H. Williams

J. Phys. Chem. B **109**, 3707-3710 (2005)

A new DFT/MM procedure is described, using higher-level calculations to correct lower level QM data on the fly, allowing calculation of kinetic isotope effects.

Surface and Volume Determination

Prediction of protein relative solvent accessibility with a two-stage SVM approach.

M.N. Nguyen and J.C. Rajapakse* [Nanyang Tech U]

Proteins **59**, 30-37 (2005)

A two-stage SVM method using PSSMs from PSI-BLAST for prediction of buried/exposed-ness is trained on 30 structures and achieves an accuracy of 90% on the Manesh and RS126 datasets (total 341 structures), outperforming other published results (85-89%). The method has been made available from a webserver.

An amino acid has two sides: A new 2D measure provides a different view of solvent exposure.

T. Hamelryck* [U Copenhagen]

Proteins **59**, 38-48 (2005)

Introduction of a directionality along $C\alpha$ - $C\beta$ axis (roughly) the in residue exposure by means of 'Half-Sphere exposure', leads to predictions that correlate better with mutant stabilities and are more conserved within protein families than other measures, and can be derived from $C\alpha$ -only models.

3. JOURNAL REVIEWS

Journal of Computational Chemistry 26(6), April 30, 2005

- 523-531 **Fitting complex potential energy surfaces to simple model potentials: Application of the simplex-annealing method.** R.A. Bustos Marín, E.A. Coronado, and J.C. Ferrero* [U Nacional Córdoba]

A combination of simplex and simulated annealing algorithms is applied to obtain globally minimum parameters for a simple function from a complex (e.g. QM) potential function.

- 532-551 **The behavior of transition metal nitrido bonds towards protonation rationalized by means of localized bonding schemes and their weights.** V. Bachler* [Max-Planck-Inst]

Electronic structure in triple bonds between transition metals and N is analyzed to evaluate their protonation potentials.

- 552-560 **Double proton transfer and one-electron oxidation behavior in double H-bonded glycine-glycine complex in the gas phase.** P. Li and Y. Bu* [Qufu Normal U]

QM analysis indicates that protons are transferred in concert rather than sequentially.

- 561-568 **Computational methods for the study of enzymic reaction mechanisms III: A perturbation plus QM/MM approach for calculating relative free energies of protonation.** P.L. Cummins and J.E. Gready* [Australian National U]. See **Methodology, QM/MM.**
- 569-583 **Electronic structure study of the initiation routes of the dimethyl sulfide oxidation by OH.** N. González-García, À. González-Lafont* [U Autònoma de Barcelona], and J.M. Lluch
- Dimethylsulfoxide can be oxidized via proton abstraction, addition-elimination, or a concerted mechanism, each of which leads to different products, according to QM studies of the potential energy surface.
- 584-598 **Magic number silicon dioxide-based clusters: Laser ablation-mass spectrometric and density functional theory studies.** Q. Kong, .L. Zhao, W. Wang, C. Wang, C. Xu, W. Zhang, L. Liu, K. Fan, Y. Li, and J. Zhuang* [Fudan U]
- Silica clusters with 4 or 8 SiO₂ groups dominate the mass spectrum in laser ablation of porous siliceous materials due to geometrical advantages of their respective clusters, according to DFT simulations.
- 599-605 **Accuracy and efficiency of atomic basis set methods versus plane wave calculations with ultrasoft pseudopotentials for DNA base molecules.** P. Pulay* [U Arkansas], S. Saebo, M. Malagoli, and J. Baker
- Gaussian basis sets are much more efficient than the plane-wave ultrasoft pseudopotential DFT method for calculating energies of DNA base structural changes, and more accurate for dihedral angles and vibrational frequencies.
- 606-611 **Theoretical insights into the mechanism of acetylcholinesterase-catalyzed acylation of acetylcholine.** T. K. Manojkumar, C. Cui, and K.S. Kim* [Pohang U Sci Tech]
- In the process of hydrolysis, acylation of the acetyl group in ACh by an AChE Ser requires the formation of transition states with short strong hydrogen bonds to the Ser and a His, as well as intermediate states where the hydrogen bond to the Ser is not as strong.
- 612-618 **The OH + CH₃SH reaction: Support for an addition-elimination mechanism from ab initio calculations.** P.L. Muiño* [Saint Francis U]
- Free radical extraction of the sulfhydryl hydrogen occurs by OH addition followed by H₂O elimination according to QM.
- 619-632 **Attaining exponential convergence for the flux error with second- and fourth-order accurate finite-difference equations. I. Presentation of the basic concept and application to a pure diffusion system.** M. Rudolph* [Friedrich-Schiller-U]
- The flux in Fick's second law can be estimated with much better precision than the local concentrations because it is an integral. Numerical integration super-converges.
- 633-641 **Attaining exponential convergence for the flux error with second- and fourth-order accurate finite-difference equations. II. Application to systems comprising first-order chemical reactions.** M. Rudolph* [Friedrich-Schiller-U]
- Kinetic-diffusion equations are also superconvergent, with even faster convergence for kinetic-limited diffusion-reaction situations.
- 642-650 **Theoretical study for the reaction of CH₃OCl with Cl atom.** H.-Q. He, J.-Y. Liu, Z.-S. Li* [Jilin U], and C.-C. Sun

In the polar stratosphere at low temperatures, extraction of Cl from CH₃OCl by a Cl atom is probably as common as extraction of H.

Journal of Computational Chemistry 26(7), May, 2005

- 651-660 **Estimation of the absolute internal-rotation entropy of molecules with two torsional degrees of freedom from stochastic simulations.** E. Darian, V. Hnizdo* [NIOSH], A. Fedorowicz, H. Singh, and E. Demchuk

Configurational entropy and a kinetic contribution can be combined to obtain a good estimate of internal entropy, as confirmed for model systems stilbene and propane with MC simulations.

- 661-667 **Agreement between experiment and hybrid DFT calculations for OH bond dissociation enthalpies in manganese complexes.** M. Lundberg* [Stockholm U] and P.E.M. Siegbahn

Hybrid functionals like B3LYP are necessary to get proper OH splitting energies (within 3 kcal/mol) for Mn complexes such as the photosystem II. BLYP consistently underestimates OH bond strength by 20 kcal/mol.

- 668-681 **Relative contributions of desolvation, inter- and intramolecular interactions to binding affinity in protein kinase systems.** P.A. Sims, C.F. Wong* [U Missouri], D. Vuga, J.A. McCammon, and B.M. Sefton. See **Applications, Enzyme Catalysis.**

- 682-690 **Empirical force-field assessment: The interplay between backbone torsions and noncovalent term scaling.** E.J. Sorin and V.S. Pande* [Stanford U]. See **Methodology, Potentials and Parameters.**

- 691-698 **A simple method for faster nonbonded force evaluations.** M.-Y. Shen and K.F. Freed* [U Chicago]. See **Methodology, Molecular Dynamics.**

- 699-707 **Fluctuating charge normal modes: An algorithm for implementing molecular dynamics simulations with polarizable potentials.** L.R. Olano and S.W. Rick* [U New Orleans]. See **Methodology, Potentials and Parameters.**

- 708-715 **A sparse algorithm for the evaluation of the local energy in quantum Monte Carlo.** A. Aspuru-Guzik* [U Calif Berkeley], R. Salomón-Ferrer, B. Austin, and W.A. Lester Jr.

Significant speedups were obtained with a new sparse matrix algorithm. The cost of evaluating the Slater determinate scales linear with system size, according to calculations with up to 390 electrons.

- 716-724 **Development of a force field for Li₂SiF₆.** A. Liivat, A. Aabloo, and J.O. Thomas* [Uppsala U]. See **Methodology, Potentials and Parameters.**

- 725-737 **An improved nucleic acid parameter set for the GROMOS force field.** T.A. Soares, P.H. Hünenberger, M.A. Kastenholz, V. Kräutler, T. Lenz, R.D. Lins, C. Oostenbrink, and W.F. van Gunsteren* [Swiss Fed Inst Tech]. See **Methodology, Potentials and Parameters.**

- 738-742 **Exploring the potential energy surface of retinal, a comparison of the performance of different methods.** F. Blomgren and S. Larsson* [Chalmers U Tech]

DFT and CASSCF produce different bond-length alternation and different twist angles associated with different charge on the Schiff base N and corresponding π bond order.

- 743-754 **New parallel software (P_Anhar) for anharmonic vibrational calculations: Application to (CH₃Li)₂.** N. Gohaud, D. Begue* [U Pau et des Pays de l'Adour], C. Darrigan, and C. Pouchan

P_Anhar calculates the vibrational spectrum using a variational algorithm. A quartic anharmonic force field, B3LYP/cc-pVTZ, is computed for methyllithium.

Journal of Molecular Modeling 11(1), February, 2005

- 1-7 **Comparative analysis of surface electrostatic potentials of carbon, boron/nitrogen and carbon/boron/nitrogen model nanotubes.** P. Politzer* [U New Orleans], P. Lane, J.S. Murray and M.C. Concha, See **Applications/ Carbon Nanoparticles**.
- 8-16 **Reasoning of spike glycoproteins being more vulnerable to mutations among 158 coronavirus proteins from different species.** G. Wu* [Dream Sci Tech Consulting] and S. Yan.
The probabilistic models were developed to analyze 158 proteins from coronaviruses in order to determine what protein is more vulnerable to mutations.
- 17-25 **Tetracycline and its analogues as inhibitors of amyloid fibrils: searching for a geometrical pharmacophore by theoretical investigation of their conformational behavior in aqueous solution.** U. Cosentino, M. Rosaria-Vari, A.A.G. Saracino, D. Pitea, G. Moro* [U Sudi di Milano-Bicocca] and M. Salmona. See **Methodology / Conformational Search and Analysis**.
- 26-40 **An extended aqueous solvation model based on atom-weighted solvent accessible surface areas: SAWSA v2.0 model.** T. Hou, W. Zhang, Q. Huang and X. Xu* [Peking U]
SAWSAv2.0 method is used to calculate the aqueous solvation free energy based on atom-weighted solvent accessible surface areas. Two different sets of atom typing rules and fitting processes for small organic molecules and proteins applied.
- 41-47 **Direct *ab initio* dynamics studies of the hydrogen abstraction reactions of hydrogen atom with *n*-propyl radical and isopropyl radical.** Q. Shu-Li* [Beijing Inst Tech], Y. Zhang and S. Zhang
Ab initio dynamics approach is used to study the kinetics of the hydrogen abstraction reactions of hydrogen atom with *n*-propyl radical and isopropyl radical.
- 48-54 **CoMFA, HQSAR and molecular docking studies of butitaxel analogues with β -tubulin.** S.L. Cunningham* [U Pittsburgh], B.W. Day and A.R. Cunningham. See **Applications / Quantitative Structural Activity Relationship**.
- 55-60 **Prediction of lower critical solution temperature of *N*-isopropylacrylamide-acrylic acid copolymer by an artificial neural network model.** H. Kay* [Hacettepe U], S. Ali-Tuncel, A. Elkamel and E. Alper. See **Applications/ Polymers**.
- 61-68 **AIPAR: *ab initio* parametrization of intermolecular potentials for computer simulations.** M.Z. Hernandes and R.L. Longo* [U Federal de Pernambuco]
Intermolecular interaction potentials between polar molecules and water are studied using *ab initio* parametrization implemented in the SJBR program.
- 69-79 **Molecular dynamics simulations of the human CAR ligand-binding domain: deciphering the molecular basis for constitutive activity.** B. Windshügel* [Martin-Luther U], J. Jyrkkärinne, A. Poso, P. Honkakoski, and W. Sippl. See **Applications Comparative/Homology Modeling**.

80-86 **Analysis of the interactions of ribonuclease inhibitor with kanamycin.** Z. Wang, L. Zhang, J. Lu* [Health Sci Cent of Peking U] and L. Zhang. See **Applications/Protein-Protein interactions.**

108-113 **Modeling of the phase equilibria of polystyrene in methylcyclohexane with semi-empirical quantum mechanical methods I.** H.W. -Wachnik* [Warsaw U] and S.Ó. Jónsdóttir.

Interaction energies are determined for three molecular pairs, the solvent and the model molecule, two solvent molecules and two model molecules, and used to calculate UNIQUAC interaction parameters, a_{ij} and a_{ji} .

Journal of the American Chemical Society 127(9-13), 2005

2808-2809 **Deblurred observation of the molecular structure of an oil-water interface,** H. S. Ashbaugh, L. R. Pratt, M. E. Paulaitis* [Johns Hopkins U], J. Clohery, and T. A. Beck, [MD and MC simulation study the structure at a carbon / water interface]

2888-2899 **Isotope effects, dynamics, and the mechanism of solvolysis of aryldiazonium cations in water,** B. R. Ussing, and D. A. Singleton* [Texas A&M U], [Quasi-classical dynamics and DFT simulation]

3191-3197 **Origin of tight binding of a near-perfect transition-state analogue by cytidine deaminase: Implications for enzyme catalysis,** H. Guo, N. Rao, Q. Xu, and H. Guo* [U Tn], [QM/MM simulation using a fast semi-empirical DFT approach is tested against high level QM]

3531-3544 **Spectroscopy and density functional studies of the red copper site in nitrosocyanin: Role of the protein in determining active site geometric and electronic structure,** L. Basumallick, R. Sarangi, S. D. George, B. Elmore, A. B. Hooper* [U Mn], B. Hedman, K. O. Hodgson, and E. I. Solomon* [Stanford U], [DFT supplement CD, Raman and X-ray adsorption spectroscopies]

3589-3595 **Limited flexibility of lactose detected from residual dipolar couplings using molecular dynamics simulations and steric alignment methods,** M. Martin-Pastor* [CSIC], A. Canales, F. Corzana, J. L. Asensio, and J. Jimenez-Barbero* [CSIC], [MD simulations give insight into NMR data on lactose]

3624-3634 **Computational rationalization of the dependence of the enantioselectivity on the nature of the catalyze in the vanadium-catalyzed oxidation of sulfides by hydrogen peroxide,** D. Balcells, F. Maseras* [U Auto Barcelona], and G. Ujaque, [IMOMM calculations at the DFT:MM3 are performed]

3688-3689 **Dienophile twisting and substituent effects influence reaction rates of intramolecular Diels-Alder cycloadditions: A DFT study,** K. S. Khuong* [UCLA], C. M. Beaudry, D. Trauner, and K. N. Houk* [UCLA], [DFT study of the Diels-Alder reaction]

3807-3816 **Homolysis of weak Ti-O bonds: Experimental and theoretical studies of titanium oxygen bonds derived from stable nitroxyl radicals,** K.-W. Huang, J. H. Han, A. P. Cole, C. B. Musgrave, and R. M. Waymouth* [Stanford U], [DFT and experiment combine to study titanium-oxygen interaction]

3952-3963 **Solvent effects on the vibrational activity and photodynamics of the green fluorescent protein chromophore: A quantum-chemical study,** P. Altoe, F. Bernardi, M. Garavelli* [U Bologna], G. Orlandi, and F. Negri* [U Bologna], [High level QM (CASSCF) probes photoreaction paths]

3964-3972 **A theoretical study on the origin of π -facial stereoselectivity in the alkylation of enolates derived from 4-substituted γ -butyrolactones,** K. Ando* [U Ryukyus], [Alkylation studied with QM at various high levels of theory]

4021-4032 **Ruthenium(II)-catalyzed hydrogenation of carbon dioxide to formic acid. Theoretical study of real**

- catalyst, ligand effects, and solvation effects**, Y. Ohnishi, T. Matsunaga, Y. Nakao, H. Sato, and S. Sakaki* [Kyoto U], [DFT and MP4(SDQ) methods applied to real ruthenium catalysts]
- 4042-4048 **Toward understanding mobile proton behavior from first principles calculation: The short hydrogen bond in crystalline urea-phosphoric acid**, C. A. Morrison* [U Edinburgh], M. M. Siddick, P. J. Camp, and C. C. Wilson, [Plane wave DFT MD simulation with VASP]
- 4091-4103 **Factors governing the substitution of La³⁺ for Ca²⁺ and Mg²⁺ in metalloproteins: A DFT/CDM study**, T. Dudev, L.-Y. Chang, and C. Lim* [Acad Sinica], [DFT with continuum dielectric methods probe the substitution of lanthanides for divalent ions in holoproteins]
- 4162-4163 **Electronic structures and properties of twisted polyacenes**, J. E. Norton, and K. N. Houk [UCLA]
- 4232-4241 **Hybrid QM/MM and DFT investigations of the catalytic mechanism and inhibition of the dinuclear zinc metallo- β -lactamase CcrA from *Bacteroides fragilis***, H. Park, E. N. Brothers, and K. M. Merz, Jr.* [Penn State U], [QM/MM at the PM3 level after docking of nitrocefin with AutoDock]
- 4242-4253 **A comparative study of the catalytic mechanisms of the zinc and cadmium containing carbonic anhydrase**, T. Marino, N. Russo* [U Calabria], and M. Toscano, [High level DFT calculations on simple model systems]
- 4354-4371 **Syntheses and structures of hypervalent pentacoordinate carbon and boron compounds bearing an anthracene skeleton – Elucidation of hypervalent interaction based on X-ray analysis and DFT calculation**, M. Yamashita, Y. Yamamoto* [Hiroshima U], K. Akiba* [Waseda U], D. Hashizume, F. Iwasaki, N. Takagi, and S. Nagese, [X-ray and DFT characterized novel pentacoordinate and tetracoordinate carbon and boron compounds with an anthracene skeleton]
- 4403-4415 **The electronic structure of the isoelectric, square-planar complexes [Fe^{II}(L)₂]²⁻ and [Co^{III}(L^{Bu})₂]⁻ (L²⁻ and (L^{Bu})²⁻ = benzene-1,2-dithioates): An experimental and density functional theoretical study**, K. Ray, A. Begum, T. Weyhermuller, S. Piligkos, J. Van Slageren, F. Neese* [U Stuttgart], and K. Wieghardt* [U Stuttgart], [DFT and spectroscopy probe two formally isoelectronic transition-metal dithiolato complexes]
- 4445-4453 **Water-promoted hydrolysis of a highly twisted amide: Rate acceleration caused by the twist of the amide bond**, J. I. Majika, J. M. Mercero, and X. Lopez* [Euskal Herriko U], [DFT calculations with a SCI-PCM solvation model probe amide hydrolysis]
- 4490-4496 **Viscosity of the aqueous liquid/vapor interfacial region: 2D electrochemical measurements with a piperidine nitroxy radical probe**, D. G. Wu, A. D. Malec, M. Head-Gordon, and M. Majda* [UC Berkeley], [Electronic structure calculations aid experiment by probing water interactions with the solute]
- 4640-4648 **Unexpected relative aqueous solubilities of a phosphotyrosine analogue and two phosphonate derivatives**, S. Boresch* [U Wien], M. Leitgeb, A. Beselman, and A. D. MacKerell, Jr.* [U Md], [Force field development and FEP are performed to investigate the relative solubilities of phosphotyrosines]
- 4722-4729 **Elucidating the vibrational spectra of hydrogen-bonded aggregates in solution: Electronic structure calculations with implicit solvent and first-principles molecular dynamics simulations with explicit solvent for 1-hexanol in *n*-hexane**, J. M. Stubbs, and J. I. Siepmann* [U Mn], [Car-Parrinello MD, classical MD and MC simulation probe the vibrational spectra of monomers through pentamers of 1-hexanol]
- 4959-4964 **Molecular dynamics simulation study on a monolayer of half [2]rotaxane self-assembled on Au(111)**, Y. H. Jang, S. S. Jang, and W. A. Goddard* [Cal Tech], [A Dreiding FF with Mulliken DFT derived charges probes the interaction of rotaxane with an *fcc* gold surface in short MD simulation]

Journal of Chemical Theory and Computation 1(2), March 2005

Dynamics

- 181-193 **Computational ^{59}Co NMR spectroscopy: Beyond static molecules.** S. Grigoleit and M. Bühl* [Max-Planck]

^{59}Co NMR chemical shifts are computed using both static calculations with equilibrium geometries as well as dynamic methods for calculating zero-point and classical thermal effects.

- 194-200 **Understanding the cosolvation effect of dendrimers.** G. Teobaldi, M. Melle-Franco, and F. Zerbetto [U Bologna]

New MD simulation results for dendrimers of polypropylene amine in CH_2Cl_2 quantitatively reproduce the cosolvation effect.

- 201-207 **Direct dynamics studies on the hydrogen abstraction reactions of an F atom with CH_3X (X = F, Cl, and Br).** L. Wang, J-Y Liu, Z-S Li* [Jilin U], and C-C Sun

Activation energies for hydrogen abstraction reactions of $\text{F} + \text{CH}_3\text{F}$ (R1), $\text{F} + \text{CH}_3\text{Cl}$ (R2), and $\text{F} + \text{CH}_3\text{Br}$ (R3) are on the order of $R1 > R2 > R3$ and the rate constants exhibit just the opposite order of $k3 > k2 > k1$.

Statistical Mechanics

- 208-214 **Hierarchical numerical solution of Smoluchowski equations with rough potentials.** P. Banushkina and M. Meuwly* [U Basel]

“We present an efficient and numerically robust algorithm to follow diffusive processes on rough potential energy surfaces.”

Quantum Chemistry

- 215-229 **A theoretical study on the factors influencing cyanine photoisomerization: The case of thiacyanine in gas phase and in methanol.** R. Improta and F. Santoro* [CNR Pisa]

“The effects influencing cyanine photoisomerization on the S1 surface in the condensed phase have been investigated by an integrated quantum mechanical approach, focused mainly on 3,3'-diEt-2,2'-thiacyanine.”

- 230-238 **Ab initio and DFT conformational studies of propanal, 2-butanone, and analogous imines and enamines.** H. Zhong, E.L. Stewart, M. Kontoyianni, and J.P. Bowen* [U North Carolina]

Calculation of the PES suggests that there are two minima for each of the molecules listed above with the exception of 2-butanone, which shows three distinct minima.

- 239-247 **Theoretical surface spectroscopy of NO on the Pt(111) surface with the DAM (Dipped Adcluster Model) and the SAC-CI (Symmetry-Adapted-Cluster Configuration-Interaction) method.** H. Nakatsuji* [Kyoto U], N. Matsumune, and K. Kuramoto

Structures, absorption sites, absorption energies and K-shell binding energies of NO adsorbates on a Pt(111) surface are modeled.

- 248-254 **Pseudospectral local second-order Moller-Plesset methods for computation of hydrogen bonding energies of molecular pairs.** G.A. Kaminski* [Central Michigan U], J.R. Maple, R.B. Murphy, D.A. Braden, and R.A. Friesner

An extrapolation protocol is used to compute binding energies of molecular dimers.

- 255-260 **Connecting Pauling and Mulliken electronegativities.** D.R. Herrick [U Oregon]

A new conversion formula is derived analytically from the classic valence bond model.

- 261-266 **An examination of basis set superposition error at the correlated level: Illuminating the role of the exchange repulsion.** C.S. Nash [U New England]

A new counterpoise procedure is presented.

- 267-278 **Functional group basis sets.** B.G. Janesko and D. Yaron* [Carnegie Mellon]

Functional group-specific basis sets are used to decrease computational expense.

- 279-285 **The perfluoroadamantyl radicals C10F15 and their anions.** X-J Feng, Q-S Li* [Beijing Instit Tech], Y. Xie, and H.F. Schaefer III* [U Georgia]

Optimized geometries, electron affinities, and harmonic vibrational frequencies of perfluoroadamantyl radicals are calculated using DFT methods.

Reaction mechanisms

- 286-298 **Activation of H-H, C-H, C-C and C-Cl bonds by Pd and PdCl-. Understanding anion assistance in C-X bond activation.** A. Diefenbach, G.T. de Jong, and F.M. Bickelhaupt* [Vrije U]

“Mechanistic pathways for oxidative addition of Pd and PdCl- to H₂ (H-H), CH₄ (C-H), C₂H₆ (C-C and C-H) and CH₃Cl (C-Cl) were studied uniformly at the ZORA-BP86/TZ(2)P level of relativistic nonlocal density functional theory (DFT).”

Nanochemistry

- 299-306 **Melting-like transition in a ternary alkali nanoalloy: Li₁₃Na₃₀Cs₁₂.** A. Aguado and J.M. López [U Valladolid]

A theoretical analysis of the equilibrium geometry and thermal behavior of the ternary Li₁₃Na₃₀Cs₁₂ alkali nanoalloy is presented.

Polymers and biopolymers

- 307-314 **Linear and nonlinear optics properties of polyphosphazene/polynitrile alternating copolymers.** D. Jacquemin [U Notre-Dame]

An oligomeric approach is used to study the optical properties of the title copolymers.

Biomolecular systems

- 315-324 **Molecular dynamics simulations of HIV-1 protease suggest different mechanisms contributing to drug resistance.** F. Wartha, A.H.C. Horn, H. Meiselbach, and H. Sticht* [Friedrich-Alexander U Erlangen-Nurnberg]

MD simulations of an active site mutation provide an explanation for drug resistance.

- 325-336 **Electrostatic polymer condensation and the A/B polymorphism in DNA: Sequence effects.** A.K. Mazur [CNRS]
 “Dynamics of the polymorphic AB transitions in DNA is compared for two polypurine sequences, poly(dA).poly(dT) and poly(dG).poly(dC).”
- 337-344 **Theoretical study of the antioxidant activity of vitamin E: Reactions of α -tocopherol with the hydroperoxy radical.** M. Navarrete, C. Rangel, J. Espinosa-García, and J.C. Corchado* [U Extremadura]
 Hydrogen abstraction from the phenolic hydrogen and hydroperoxy addition to the aromatic ring of α -tocopherol are studied using transition state theory.

Journal of Physical Chemistry B 109 (5-13), 2005

- 1822-1833 **A study of pore blockage in silicalite zeolite using free energy perturbation calculations,** A. Gupta, and R. Q. Snurr* [Northwestern U], [Zeolites with large coadsorbed molecules such as *n*-hexane, cyclohexane or benzene, compared to smaller penetrants (methane) are simulated to understand the free energy paths and rates for methane hopping past the larger co-adsorbates]
- 1936-1946 ***n*-heptane under pressure: Structure and dynamics from molecular simulations,** M. Krishnan, and S. Balasubramanian* [JNCASR], [PBC MD simulations are performed at pressures ranging from 1-70 kbar]
- 1959-1969 **Simple energy landscape model for the kinetics of functional transitions in proteins,** O. Miyashita, P. G. Wolynes, and J. N. Onuchic* [UCSD], [A iterative usage of normal mode calculations shows the conformational changes (and non-linearity) between two switched energy surfaces as a ligand is (un)bound]
- 2007-2013 **Binding of charged ligands to macromolecules. Anomalous salt dependence,** F. L. B. da Siva* [Lund U], S. Linse, and B. Jonsson, [Charged macromolecules are shown to alter binding to receptors in an unexpected way as verified by MC simulations with a dielectric continuum model]
- 2014-2020 **Pressure-induced ordering in adamantane: A Monte Carlo simulation study,** N. A. Murugan, and S. Yashonath* [IIS], [NPT-ensemble MD is performed in variable shaped simulation cells]
- 2949-2955 **Hydrogen-bond dynamics in the air-water interface,** P. Liu, E. Harder, and B. J. Berne* [Columbia U], [MD looks at dynamics of hydrogen bond formation and breakage at the air-water interface including polarization with the fluctuating charge model]
- 2985-2994 **Tests of an approximate scaling principle for dynamics of classical fluids,** T. Young, and H. C. Andersen* [Stanford U], [MD tests the scaling principle that two equilibrium liquids will have very similar dynamical properties if they have the same density and similar pair correlation functions]
- 2995-3007 **Molecular dynamics assignment of NMR correlation times to specific motions in a “basket-handle porphyrin” heme,** R. Popescu, J. Mispelter, J. Gallay, and L. Mouawad* [U Paris-Sud], [MD order parameters compare well to NMR data]
- 3065-3070 **Quantum chemical evaluation of protein control over heme ligation: CO/O₂ discrimination in myoglobin,** F. De Angelis, A. A. Jarzecki, R. Car, and T. G. Spiro* [Princeton U], [Car-Parrinello DFT calculations looks at the 13 closest residues to the heme]
- 3446-3453 **Molecular dynamics study of hydrated Faujasite-type zeolites,** K. Shirono, A. Endo, and H. Daiguji* [U Toyko], [MD simulation of hydrated NaX where X is Si/Al = 1.0 or NaY, Si/Al = 2.0).

- 3531-3538 **Atomistic simulation of a nematogen using a force field derived from quantum chemical calculations**, I. Cacelli, G. Prampolini* [U Pisa], and A. Tani, [Bulk phase MD simulations on 4-*n*-pentyl-4'-cyanobiphenyl]
- 3539-3545 **Adsorption of NH₃ and H₂O in acidic chabazite. Comparison of ONIOM approach with periodic calculations**, X. Solans-Monfort, M. Sodupe* [U Auto Barcelona], V. Branchadell, J. Sauer, R. Orlando, and P. Ogliengo, [B3LYP/semi-empirical ONIOM calculations of clusters vs. periodic Si/Al 11/1 chabazite]
- 3546-3552 **Drying and hydrophobic collapse of paraffin plates**, X. Huang, R. Zhou, and B. J. Berne* [Columbia U], [MD looks at the drying transition between two hydrophobic plates]
- 3553-3564 **Solvation dynamics in acetonitrile: A study incorporating solute electronic response and nuclear relaxation**, F. Ingrosso, B. M. Ladanyi* [U Pisa], B. Mennucci, M. D. Elola, and J. Tomasi, [PCM on the solute and MD in solvent of coumarin 153 in acetonitrile]
- 3565-3574 **MST continuum study of the hydration free energies of monovalent ionic species**, C. Curutchet, A. Bidon-Chanal, I. Soteras, M. Orozco* [U Barcelona], and F. Javier Luque* [U Barcelona], [A continuum model defining the cavity between solute and solvent for predicting hydration free energies is tested and shown to have an error of less than 5%]
- 3586-3593 **Intraresidue distribution of energy in proteins**, B. Trebbi, M. Fanti, I. Rossi, and F. Zerbetto* [U Bologna], [Testing the question of whether intraresidue energy distributions follow a Boltzmann distribution]
- 3603-3615 **Calculating absorption shifts for retinal proteins: Computational challenges**, M. Wanko, M. Hoffmann, P. Strodel, A. Koslowski, W. Thiel, F. Neese, T. Frauenheim, and M. Elstner* [U Paderborn], [A procedure combining structure optimization or MD using DFT with a semi-empirical or ab initio multireference CI treatment of excitation energies is applied]
- 3616-3626 **DFT/electrostatic calculations of pK_a values in cytochrome *c* oxidase**, D. Popovic, J. Quenneville, and A. A. Stuchebrukhov* [UC Davis], [pK_a values for two redox states of the protein are estimated]
- 3627-3638 **Magnetic effects of disulfide bridges: A density function and semiempirical study**, F. Sirockin, and A. Dejaegere* [CNRS], [DFT chemical shielding calculations show significant contributions from disulfide bridges at distances regularly sampled in protein structures]
- 3681-3689 **Effect of solvent upon CH-O hydrogen bonds with implications for protein folding**, S. Scheiner* [Utah State U], and T. Kar [DFT and HF calculations look at CH-O hydrogen bonds between water and CF_{*n*}H_{4-*n*} with *n* = 0-3]
- 3780-3786 **Molecular dynamics simulations on the effects of diameter and chirality on hydrogen adsorption in single walled carbon nanotubes**, H. Cheng* [Air Prod Chem Inc], A. C. Cooper, G. P. Pez, M. K. Kostoc, P. Piotrowski and S. J. Stuart* [Clemson U], [MD of hydrogen storage in nanotubes]
- 3915-3920 **Analytic potential energy functions for simulating aluminum nanoparticles**, A. W. Jasper, N. E. Schultz, and D. G. Truhlar* [U Mn], Potential energy functions are parameterized to a limited set of cluster and bulk data prove better at representing nanoscale particles]
- 4123-4128 **Hydroxyl radical in aqueous solution: Computer simulation**, I. M. Svishchev* [Trent U], and A. Y. Plugatyr, [MD with SPC/E and a simple point charge model for the hydroxyl radical at multiple temperatures]
- 4162-4167 **Mapping the backbone dihedral free-energy surfaces in small peptides in solution using adiabatic free-energy dynamics**, L. Rosso, J. B. Abrams, and M. E. Tuckerman* [NYU], [The adiabatic free-energy dynamics is applied to di- and tri-peptides in the gas phase in the context of the CHARMM22 force field]

- 4172-4180 **A modified Poisson-Boltzmann model including charge regulation for the adsorption of ionizable polyelectrolytes to charged interfaces, applied to lysozyme adsorption on silica**, P. Maarten Biesheuvel* [Wageningen U], M. van der Veen, and W. Norde, [A modified PB method is described that treats both the polymer and the interface (with a mean field electrostatic potential normal to the surface)]
- 4215-4226 **A minimal model of three-state folding dynamics of helical proteins**, A. Stizza, E. Capriotti, and M. Compiani* [U Camerino], [A diffusion-collision-like model is developed]
- 4269-4278 **Molecular dynamics simulation of swollen membrane of perfluorinated ionomer**, S. Urata* [Asahi Glass Co], A. Takada, W. Shinoda, S. Tsuzuli, and M. Mikami, [MD simulations of poly(tetrafluoroethylene) backbones and perfluorosulfonic side chains under varying water contents]
- 4520-4532 **Self-assembly of small polycyclic aromatic hydrocarbons on graphite: A combined scanning tunneling microscopy and theoretical approach**, G. M. Florio, T. L. Werblowsky, T. Muller, B. J. Berne* [Columbia U], and G. W. Flynn* [Columbia U], [DFT aids in the interpretation of STM images]
- 4700-4706 **Capillary condensation in a geometrically and a chemically heterogeneous pore: A molecular simulation study**, J. Puibasset* [CNRS], [An extended Gibbs ensemble MD technique probes geometric and chemical disorder of fluids in a confined media]
- 4717-4725 **Atomistic modeling of crystal-to-amorphous transition and associated kinetics in the Ni-Nb system by molecular dynamics simulations**, X. D. Dai, J. H. Li, and B. X. Liu* [Tsinghua U], [Ab initio calculations facilitate the development of a β -bond potential for Ni-Nb]
- 4731-4737 **Hierarchical modeling N₂ adsorption on the surface of and with a C₆₀ crystal: From quantum mechanics to molecular simulation**, J. Jiang* [U Delaware], J. B. Klauda, and S. I. Sandler, [QM hybrid interaction energy methods and GCMC methods look at fairly tightly packed C₆₀ crystals]
- 4738-4747 **Cation mobility and the sorption of chloroform in zeolite NaY: Molecular dynamics study**, N. A. Ramsahye, and R. G. Bell* [RIGB], [MD simulations at multiple temperatures follow cation migration upon chloroform sorption in a zeolite]
- 5012-5020 **DFT vibrational calculations of rhodamine 6G adsorbed on silver: Analysis of tip-enhanced Raman spectroscopy**, H. Watanabe, N. Hayazawa, Y. Inouye* [Osaka U], and S. Kawata, [DFT allows assignment of near-field Raman bands]
- 5199-5206 **[2+2] cycloaddition reactions of ethylene derivatives with the Si(100)-2x1 surface: A theoretical study**, Y. Wang, J. Ma* [Nanjing U], S. Inagaki, and Y. Pei, [DFT and MP2 theory]
- 5259-5266 **Theoretical study of general base-catalyzed hydrolysis of aryl esters and implications for enzymatic reactions**, J. Xie, D. Xu, L. Zhang, and H. Guo* [U New Mexico], [DFT with a polarized continuum model are applied]
- 5331-5340 **Theoretical study of internal field effects on peptide amide I modes**, H. Lee, S.-S. Kim, J.-H. Choi, and M. Cho* [Korea U], [Ab initio calculations are performed on di- and tri-peptide models]
- 5348-5357 **Ab initio modeling of amide I coupling in antiparallel β -sheets and the effect of ¹³C isotopic labeling on infrared spectra**, P. Bour* [Acad Sci Czech Rep], and T. A. Keiderling* [U Illinois], [DFT, force fields and ab initio calculations investigate amide I structure in β -sheets]
- 5368-5374 **Vapor-liquid and vapor-solid phase equilibria for united-atom benzene models near their triple points: The importance of quadrupolar interactions**, X. S. Zhao, B. Chen, S. Karaborni, and J. I. Siepmann* [U Minn], [Gibbs ensemble MC simulations are applied with united-atom force fields]

- 5421-5424 **Topological defects and bulk melting of hexagonal ice**, D. Donadio* [ETH], P. Raiteri, and M. Parrinello, [Classical MD and "metadynamics" show melting in hexagonal ice]
- 5541-5547 **Mesostructures of cobalt nanocrystals. I. Experiment and theory**, V. Germain, J. Richardi, D. Ingert, and M. P. Pileni* [U Pierre et Marie Curie], [Experiment and theory study cobalt nanocrystals]
- 5574-5579 **Theoretical study on the photophysical properties of hexapyrrolidine C₆₀ adducts with Th, D3, and S6 symmetries**, X.-D. Li, W.-D. Cheng* [Chinese Acad Sci], D.-S. Wu, Y.-Z. Lan, H. Zhang, Y.-J. Gong, F.-F. Li, and J. Shen, [DFT and higher level calculations probe C₆₀ geometries]
- 5684-5690 **Structure and energetics of water-silanol binding on the surface of silicalite-1: Quantum chemical calculations**, O. Saengsawang, T. Remsungnen, S. Fritzsche, R. Haberlandt, and S. Hannongbua* [Chulalongkorn U], [Various levels of QM look at water/silanol interaction on silicalite-1]
- 5759-5765 **Liquid-vapor interface of methanol-water mixtures: A molecular dynamics study**, T.-M. Chang* [U Wisc], and L. X. Dang, [A polarizable force field is applied to methanol-water mixtures in MD]
- 5855-5872 **Monte Carlo simulations of the solution structure of simple alcohols in water-acetonitrile mixtures**, P. I. Nagy* [U Toledo], and P. W. Erhardt, [MD explores the ethyl, isopropyl, isobutyl and tertiary butyl alcohols in water, acetonitrile and mixtures of the two solvents]
- 5895-5902 **Ab initio molecular dynamics simulation of a room temperature ionic liquid**, M. G. Del Popolo, R. M. Lynden-Bell, and J. Kohanoff* [Cambridge U], [DFT ab initio MD simulations are performed on dimethyl imidazolium chloride]
- 5919-5926 **Theoretical study of the effect of water in the process of proton transfer of glycineamide**, Y. Sun, H. Li* [Zhejiang U], W. Liang, and S. Han, [DFT investigates the tautomerism from glycineamide to glycineamic acid]
- 5945-5949 **Influence of the water molecule on cation- π interaction: An ab initio second order Moller-Plesset perturbation (MP2) calculation**, Y. Xu, J. Shen* [Chinese Acad Sci], W. Zhu* [Chinese Acad Sci], X. Luo, K. Chen, and H. Jiang* [Chinese Acad Sci], [Water interaction with a methylammonium-benzene complex is probed in ab initio calculations]
- 5962-5976 **Vapor-to-droplet transition in a Lennard-Jones fluid: Simulation study of nucleation barriers using the ghost field method**, A. V. Keimark* [TRI/Princeton], and A. Vishnyakov, [MC simulations of a vapor confined to a spherical container with repulsive walls probes nucleation phenomena]
- 6052-6060 **First-principles calculation of the ¹⁷O NMR parameters of a calcium aluminosilicate glass**, M. Benoit* [CEMES], M. Profeta, F. Mauri, C. J. Pickard, and M. E. Tuckerman, [Ab initio Car-Parrinello calculations are applied to calculate NMR observables]
- 6153-6158 **Theoretical analysis of fluorine addition to single-walled carbon nanotubes: Functionalization routes and addition patterns**, G. V. Lier* [UCL], C. P. Ewels, F. Zuliani, A. De Vita, and J.-C. Charlier, [MC simulations within a Huckel model are applied along with ab initio methods]
- 6183-6192 **First-principles modeling of unpassivated and surfactant-passivated bulk facets of Wurtzite CdSe: A model system for studying the anisotropic growth of CdSe nanocrystals**, L. Manna* [INFM], L. W. Wang* [INFM], R. Cingolani, and A. P. Alivisatos, [Plane wave DFT with PEtot are applied with pseudopotentials for CdSe growth]
- 6304-6310 **Theoretical study of the adsorption and dissociation of oxygen on Pt(111) in the presence of a homogeneous electric fields**, M. P. Hyman, and J. W. Medlin* [U Colorado], [DFT calculations oxygen on platinum surfaces in the presence of positive or negative electric fields]

- 6355-6365 **Relative permittivity of polar liquids. Comparison of theory, experiment, and simulation**, M. Valisko* [U Veszprem], and D. Boda, [A dipolar hard sphere fluid model including polarizability based on perturbation theory using their Kirkwood g-factor is applied]
- 6386-6396 **Diffusion of alkane mixtures in zeolites: Validating the Maxwell-Stefan formulation using MD simulations**, R. Krishna* [U Amsterdam], and J. M. van Baten, [Binary, ternary and quaternary mixtures including methane, ethane, propane and n-butane in FAU zeolite with MD and CBMC]
- 6397-6404 **Sedimentation equilibrium of colloidal suspensions in a planar pore based on density functional theory and the hard-core attractive Yukawa model**, S. Zhou* [Zhuzhou Inst Tech], and H. Sun, [DFT of a hard-core attractive Yukawa fluid in a gravitational field]
- 6405-6415 **Molecular dynamics simulation of aqueous NaF and NaI solutions near a hydrophobic surface**, S. Pal* [Intl U Bremen], and F. Muller-Plathe* [Intl U Bremen], [MD of alkali halide salts and water as a function of distance from a hexagonal hole in an alkane crystal]
- 6416-6421 **Mechanisms of initial propane activation on molybdenum oxides: A density functional theory study**, G. Fu, X. Xu* [Xiamen U], X. Lu, and H. Wan* [Xiamen U], [Six different mechanisms of C-H bond activation on metal oxides are studied with DFT]
- 6442-6447 **Non-covalent interactions between unsolvated peptides: Helical complexes based on acid-base interactions**, R. Sudha, M. Kohtani, and M. F. Jarrold* [Indiana U], [Mass spectroscopy and MD simulation combine to study peptide structure]

4. ADDRESSES OF PRINCIPAL AUTHORS

The production sites for the corresponding or principal authors are given in brackets in the citations. When not designated by the publisher, the first author is assumed to be the principal. Current addresses are listed

V.K. Agrawal
QSAR and Comp. Chem. Labs.
A.P.S. Univ.
Rewa - 486 003, India

Bruce A. Armitage
army@andrew.cmu.edu
Dept. of Chemistry
Carnegie Mellon Univ.
4400 Fifth Ave.
Pittsburgh, PA 15213, USA

Johan Aqvist
Dept. of Cell and Mol. Biol.
Uppsala Univ
Biomedical Center
Box 596, SE-751 24
Uppsala, Sweden

Alán Aspuru-Guzik
alan@aspuru.com
Kenneth S. Pitzer Center
for Theoretical Chemistry
Department of Chemistry
Univ. of California at Berkeley
Berkeley, CA 94720-1460, USA

András Aszódi
andras.aszodi@
pharma.novartis.com
Novartis IBR Vienna
Brunnerstrasse 59
A-1235 Vienna, Austria

Vinzenz Bachler
bachler@mpi-muelheim.mpg.de
Max-Planck-Institut für
Bioorganische Chemie
Stiftstrasse 34-36
Postfach 101365
D-45413 Mülheim an der Ruhr,
Germany

Biman Bagchi
bbagchi@sscu.iisc.ernet.in
Solid State and Struct. Chem.
Indian Inst. Science
Bangalore-560012, India

David Baker
dabaker@u.washington.edu
Dept. of Biochem.
Univ. of Washington
Box 357350, J-567 Health Sci.
Seattle, WA 98195-7350, USA.

Sanjoy Bandyopadhyay
sanjoy@chem.iitkgp.ernet.in
Molecular Modeling Lab.
Dept. of Chemistry
Indian Inst. Tech.
Kharagpur-721302, India

Canan Baysal
canan@sabanciuniv.edu
Lab. of Comput. Biol.
Faculty of Engg. and Nat. I Sci.
Sabanci University
Orhanli 34956
Tuzla, Istanbul, Turkey

Didier Begue
didier.begue@univ-pau.fr
Laboratoire de Chimie Structurale
UMR 5624, FR2606 IPREM
Univ. de Pau
et des Pays de l'Adour
IFR, Rue Jules Ferry, BP27540
64075 PAU Cedex, France

David Benson
dbenson@chem.wayne.edu
Dept. of Chem.
Wayne State Univ.
5101 Cass Ave.
Detroit, MI 48202, USA

P.V. Bharatam
Dept. of Med. Chem.
NIPER, Sector-67
S.A.S. Nagar
Mohali - 160 062, India

Andrea Bottoni
andrea.bottoni@unibo.it
Dept. di Chimica "G.Ciamician,"
Univ. di Bologna
via Selmi 2, 40126 Bologna, Italy.

Charles L. Brooks, III
brooks@scripps.edu
Dept. of Mol. Biol.
The Scripps Res. Inst.
10550 North Torrey Pines Rd.
La Jolla, CA 92037, USA

Yuxiang Bu
byx@sdu.edu.cn
Department of Chemistry
Qufu Normal University
Qufu 273165, PR China

M.A. Cabrera Pérez
Dept. of Drug Design
Chemical Bioactive Center
Central Univ. of Las Villas
Santa Clara, 54830 Villa Clara, Cuba

- Ivo Cacelli
ivo@deci.unipi.it
Univ. di Pisa
via Risorgimento 35
56126 Pisa, Italy
- Paolo Carloni
carloni@sissa.it
SISSA/ISAS
Via Beirut 2-4
34014 Trieste, Italy
- Sergei F. Chekmarev
chekmarc@itp.nsc.ru
Inst. Thermophysics
630090 Novosibirsk, Russia
- T.H. Chan
Dept. of Appl. Biol. & Chem. Tech.
Inst. of Mol. Tech. for Drug Disc.
and Synthesis
The Hong Kong Polytechnic Univ.
Hung Hom, Hong Kong, SAR, China
- B.W. Clare
Sch. of Biomed. & Chem. Sci.
The Univ. of Western Australia
35 Stirling Highway
Crawley WA 6009, Australia
- Mylène Compoint
Lab. de Physique Moléculaire
UMR CNRS 6624-Faculté des Sci.
la Bouloie
Université de Franche-Comté
25030 Besançon Cedex, France
- Peter B. Crowley
crowley@itqb.unl.pt
Inst. de Tecn. Quím. e Biol.
Univ. Nova de Lisboa
Av. Da República, Apartado 127
Oeiras, Portugal.
- M. V. Cubellis
cubellis@unina.it
Dept. de Chimica Biologica
Via Mezzocannone 16
80134, Napoli, Italia.
- S.L. Cunningham
scunni3@lsu.edu
Dept. of Env. & Occup. Health
Univ. of Pittsburgh
Pittsburgh, PA 15261, USA
- Andrew Dalby
a.r.dalby@exeter.ac.uk
School of Biol. and Chem. Sci.
and Eng. and Comput. Science
Univ. of Exeter
Washington Singer Lab's
Perry Road, Prince of Wales Road
Exeter EX4 4QG, UK
- Maurice de Koning
Instituto de Física
Universidade de São Paulo
Caixa Postal 66318
05315-970 São Paulo, SP, Brazil
- Marc de Jonge
marc@molmo.be
Janssen Pharma.
Antwerpsesteenweg 37
B-2350 Vosselaar, Belgium
- Tapan Desai
Dept. of Mat. Sci. and Engineering
Rensselaer Polytechnic Institute
Troy, NY 12180, USA
- Giuseppe Ermondi
giuseppe.ermondi@unito.it
Dept. di Scienza e Tecn. del Farm.
V.P. Giuria 9
I-10125 Torino, Italy.
- Dario A. Estrin
dario@qi.fcen.uba.ar
Dept. Quim. Inorg.
INQUIMAE-CONICET
Univ. de Buenos Aires
Ciudad Univ.
Pabellon II, Buenos Aires
C142EHA, Argentina
- Scott E. Feller
fellers@wabash.edu
Dept. of Chemistry
Wabash College
301 West Wabash Ave.
Crawfordsville, IN 47933, USA
- Juan C. Ferrero
jferrero@mail.fcq.unc.edu.ar
INFIQC, Dto. de Físicoquímica
Facultad de Ciencias Químicas
Universidad Nacional de Córdoba
Córdoba (5000) Argentina
- Anthony L Fink
Dept. of Chem. and Biochem.
Univ. of Calif.
Santa Cruz, CA 95064, USA
- Karl F. Freed
k-freed@uchicago.edu
The James Franck Institute
and Department of Chemistry
The University of Chicago
5640 S. Ellis Avenue
Chicago, IL 60637, USA
- Klaus Gerwert
gerwert@bph.ruhr-unibochum.de
Lehrstuhl für Biophysik
Ruhr-Univ. Bochum
D-44780 Bochum, Germany
- Valerie J. Gillet
v.gillet@sheffield.ac.uk
Dept. of Inf. Studies
Univ. of Sheffield
Regent Court, 211 Portobello Str.
Sheffield S1 4DP, UK.
- Krzysztof Ginalski
kginal@chop.swmed.edu
Dept. of Biochem.
Univ. of Texas, S.W. Med. Center
5323 Harry Hines Boulevard,
Dallas, Texas 75390-9038, USA.
- Àngels González-Lafont
angels@klingon.uab.es
Univ. Autònoma de Barcelona
08193 Bellaterra
Barcelona, Spain
- Paola Gratteri
paola.gratteri@unifi.it
Univ. Florence
via U. Schiff 6
50019 Sesto Fiorentino
Firenze, Italy
- Jill E. Gready
Jill.Gready@anu.edu.au
Computational Proteomics Group
John Curtin School of Med. Res.
Australian National University
P.O. Box 334
Canberra ACT 2601, Australia
- Thomas Hamelryck
thamelry@binf.ku.dk
Bioinf. Center
Univ. of Copenhagen
Universitetsparken 15, Bygning 10
2100 Copenhagen, Denmark
- Jenn-Kang Hwang
jkhwang@cc.nctu.edu.tw
Inst. of Bioinf.
Natl. Chiao Tung Univ.
HsinChu 30015, Taiwan
- T. Haliloglu
turkan@prc.bme.boun.edu.tr
Polymer Research Center
Bogazici University
34342 Bebek
Istanbul, Turkey
- Owen J. Hehmeyer
Dept. of Chemical Engineering
Princeton University
Princeton, NJ 08544
- Peter Werner Hildebrand
peter.hildebrand@charite.de
Inst. of Biochemistry Charité
University Medicine Berlin
10117 Berlin, Germany
- Vladimir Hnizdo
vbh5@cdc.gov
Natl. Inst. Occ. Safety & Health
M/S L-4020
1095 Willowdale Road
Morgantown, WV 26505-2888, USA
- Hans-Dieter Holtje
hoeltje@pharm.uni-duesseldorf.de
Inst. für Pharm. Chem.
Heinrich-Heine Univ. Dusseldorf
Universitätsstrasse 1
40225 Dusseldorf, Germany
- Barry Honig
Bh6@columbia.edu
HHMI and Dept. of Biochem.
and Mol. Biophys.
Columbia University
630 West 168th St
New York, NY 10032, USA
- Anders Irbäck
anders@thep.lu.se
Complex Systems Division
Dept. of Theoretical Physics
Lund University
Lund, Sweden
- Ivaylo Ivanov
iivanov@cmm.chem.upenn.edu
Dept. of Chemistry
Univ. Pennsylvania
231 South 34th St.
Philadelphia, PA 19104-6323, USA
- Matthew Jacobson
Dept. of Pharm. Chem.
University of California
San Francisco, CA 94134, USA
- Ask F. Jakobsen
MEMPHYS-Center
for Biomembrane Physics
Physics Department
University of Southern Denmark
Campusvej 55
DK-5230 Odense M, Denmark
- H. Jiang
Drug Disc. and Design Cent.
State Key Lab. of Drug Res.
Shanghai Inst. of Materia Medica
Shanghai Inst. for Biol. Sci.
Chinese Acad. of Sci.
555 Zu Chong Zhi Road
Shanghai 201203, China
- William L. Jorgensen
william.jorgensen@yale.edu
Dept. of Chemistry
Yale University
225 Prospect St.
New Haven, CT 06520, USA
- George A. Kaminski
Dept. of Chemistry
Central Michigan Univ.
Mount Pleasant, MI 48859, USA
- Martin Karplus
marci@tammy.harvard.edu
Dept. of Chem. and Chem. Bio.
Harvard Univ.
Cambridge, MA 02138, USA

Hakan Kay
hakan.kayi@chemie.uni-erlangen.de
Dept. of Chem. Engg.
Hacettepe Univ.
Beytepe, Ankara, Turkey

Yiannis Kaznessis
yiannis@cems.umn.edu
Dept. of Chem. Eng. and Mat. Sci.
Univ. of Minnesota
421 Washington Ave. SE
Minneapolis, MN 55455, USA

A. Khalafi-Nezhad
Dept. of Chem.
Fac. of Sci.
Shiraz Univ.
Shiraz 71454, Iran

Kwang S. Kim
kim@postech.ac.kr
Creative Research Initiative Center
for Superfunctional Materials
Department of Chemistry
Div. of Molecular and Life Sci.
Pohang Univ. of Science and Tech.
San 31, Hyojadong
Namgu, Pohang 790-784, Korea

Sung-Hou Kim
shkim@cchem.berkeley.edu
Dept. of Chem.
and Grad. Prog. Comp. Biochem.
Univ. of Calif.
Berkeley, CA 94720, USA

J. Klein-Seetharaman
judithks@cs.cmu.edu
Dept. of Pharmacol.
Univ. of Pittsburgh
Biomed. Sci. Tower E1058
Pittsburgh, PA 15261, USA

Edward E. Knaus
Facu. of Pharm. and Pharm. Sci.
Univ. of Alberta
Edmonton, Alberta
Canada T6G 2N8

Ming-Tat Ko
mtko@iis.sinica.edu.tw
Inst. of Inf. Science
Acad. Sinica NanKang
Taipei 115, Taiwan

Kenichiro Koga
Department of Chemistry
Okayama University
Okayama 700-8530, Japan

N. Kongkathip
NPOS Res. Unit
Dept. of Chem.
Fac. of Sci.
Kasetsart Univ.
Bangkok 10900, Thailand

Sergey Kozlov
serg@ibch.ru
Shemyakin-Ovchinnikov
Inst. of Bioorg. Chem.
Russian Acad. of Sci.
ul. Miklukho-Maklaya, 16/10
117997 Moscow, Russia.

Paul Labute
paul@chemcomp.com
Chem. Computing Group Inc.
1010 Sherbrooke St. Ste. 910
Montreal, Quebec
Canada H3A 2R7

Thierry Langer
Thierry.Langer@uibk.ac.at
Univ. Innsbruck
Innrain 52
A-6020 Innsbruck, Austria

Ronald G. Larson
rlarson@umich.edu
Chemical Engg. Department
The University of Michigan
Ann Arbor, MI 48109, USA

Sven Larsson
slarsson@chembio.chalmers.se
Dept. of Chemistry and Bioscience
Chalmers Univ. of Technology
SE-412 96 Göteborg, Sweden

Charles A. Laughton
charles.laughton@nottingham.ac.uk
Centre for Biomolecular Sci.
University of Nottingham
Nottingham NG7 2RD, UK

Maeng Eun Lee
Max-Planck-Institute
for Polymer Research
Ackermannweg 10
D-55128 Mainz, Germany

Michael S. Lee
michael.lee@amedd.army.mil
Dept. of Cell Bio. and Biochem.
U.S. Army Med. Res. Inst.
of Infect. Dis.
1425 Porter St.
Frederick, MD 21702, USA

Q. Shu Li
qsli@bit.edu.cn
State Key Lab. of Prevention
and Control of Expl. Disasters
Beijing Inst. of Tech.
Beijing, 100081, P.R. China

Ze-Sheng Li
ljiy121@mail.jlu.edu.cn
liujy121@163.com
Institute of Theoretical Chemistry
State Key Lab. of Theor.
and Comput. Chem.
Jilin University
Changchun 130023, PR China

Carmay Lim
carmay@gate.sinica.edu.tw
Inst. of Biomed. Sciences
Academia Sinica
Taipei 115, Taiwan

Wilber Lim
choonsiang.lim@yale.edu.
Department of Physics
Faculty of Science
National Univ. of Singapore
Singapore 117542

R.L. Longo
longo@ufpe.br
Dept. de Química
Fundamental
Univ. Federal de Pernambuco
50740-540 Recife, PE, Brazil

Jingfen Lu
zdsjff@bjmu.edu.cn
State Key Lab. of Natural
and Biomimetic Drugs
Health Sci. Cent. of Peking Univ.
100083 Beijing, PR China

Marcus Lundberg
marc@physto.se
Department of Physics
Stockholm University
AlbaNova University Center
SE-106 91 Stockholm, Sweden

F. Javier Luque
Javier@far1.far.ub.es
Dept. Farmacia
Unitat de Físicoquímica
Facultat de Farmacia
Univ. de Barcelona
Avgda Diagonal 643
Barcelona 08028, Spain

Kristina Luthman
Dept. of Med. Chem.
Inst. of Pharm.
Univ. of Tromsø
N-9037 Tromsø, Norway

C. J. Margulis
Dept. of Chemistry
Univ. of Iowa
319 Chemistry Bldg
Iowa City, Iowa 52242, USA

Stefan Mayewski
mayewski@biochem.mpg.de
Max Planck Inst. für Biochem.,
Abt. Strukturforschung
Am Klopferspitz 18A
82152 Martinsried, Germany

Lelio Mazzarella
lelio.mazzarella@unina.it or
mazzarella@chemistry.unina.it
Dipartimento di Chimica
Univ. degli Studi
di Napoli "Federico II"
Complesso Univ. di Monte
Sant'Angelo

Via Cynthia
80126 Napoli, Italy

Gian Pietro Miscione
Dept. di Chimica "G. Ciamician"
Univ. di Bologna
via Selmi 2
40126 Bologna, Italy

Vicent Moliner
moliner@nuvol.uji.es
Dept. Ciències Exp.
Univ. Jaume I
Box 224, 12080 Castellon, Spain

Pedro L. Muiño
pmuino@francis.edu
Department of Chemistry
Mathematics and Physical Sciences
Saint Francis University
P.O. Box 600
Loretto, PA 15940, USA

Adrian J. Mulholland
adrian.mulholland@bristol.ac.uk
School of Chemistry
Univ. of Bristol
Bristol BS8 1TS, UK

D.A. Mulholland
Nat. Prod. Res. Group
School of Chemistry
Univ. of KwaZulu-Natal
Durban 4041, South Africa

Christopher W. Murray
c.murray@astex-technology.com
Astex Technology
436 Cambridge Science Park
Milton Road
Cambridge, CB4 0QA, UK

Carlos Nieto-Draghi
Departament d'Enginyeria Química
ETSEQ
Universitat Rovira i Virgili
Avinguda dels Països Catalans 26
43007 Tarragona, Spain

Lennart Nilsson
lennart.nilsson@biosci.ki.se
Dept. of Biosci. at Novum,
Centre for Struct. Biochem.
Karolinska Inst.
SE-141 57 Huddinge, Sweden

R. Nussinov
ruthn@ncifcrf.gov
NCI-Frederick
Bldg. 469, Rm. 151
Frederick, MD 21702, USA

Mary Jo Ondrechen
mjo@neu.edu
Dept. of Chem. and Chem. Biol.
Northeastern Univ
360 Huntington Avenue
Boston, MA 02115, USA

- Modesto Orozco
modesto@mmb.pcb.ub.es
Dept. de Bioquímica i Biol. Mol.
Facultat de Química
Univ. de Barcelona
Martí i Franques 1
Barcelona, 08028, Spain
- Vijay S. Pande
pande@stanford.edu
Department of Chemistry
Stanford University
Structural Biology Dept.
and SSRL85
Stanford, CA 94305-5080, USA
- R. W. Pastor
pastor@cber.fda.gov
Lab. of Biophysics, CBER
1401 Rockville Pike
Rockville, MD 20852-1448, USA
- Josef Pánek
panek@biomed.cas.cz
MBÚ AV ČR
Videňská 1083
142 20 Praha 4, Czech Republic
and
Inst. for Molec. Biosci.
Univ. of Queensland
Brisbane, Australia
- B. Montgomery Pettitt
pettitt@uh.edu
Dept. of Chemistry
Univ. Houston
Houston, TX 77204-5641, USA
- Mónica Pickholz
monik@ifi.unicamp.br
Center for Molecular Modeling
and Chemistry Department
University of Pennsylvania
Philadelphia, PA, USA
and
Instituto de Física
Univ. Estadual de Campinas
Campinas, Brazil
- Jacob Piehler
Inst. of Biochem.
Biocenter N210
Johann Wolfgang Goethe-Univ.
Marie-Curie Straße 9
60439 Frankfurt am Main, Germany
- Piotr Pokarowski
pokar@mimuw.ed.pl
Inst. of App. Math. and Mech.
Warsaw Univ.
Banacha 2
02-097 Warsaw, Poland
- P. Politzer
ppolitz@uno.edu
Dept. of Chem.
Univ. of New Orleans
New Orleans, LA 70148, USA
- Julia V. Ponomarenko
jpon@sdsc.edu
San Diego Supercomp. Center
Univ. of Calif., San Diego
MC 0537, 9500 Gilman Drive
La Jolla, CA 92093-0537, USA
- P.L.A. Popelier
pla@umist.ac.uk
Sch. of Chem
Univ. of Manchester
Manchester M60 1QD, UK
- Clemens Posten
clemens.posten@mvm.uka.de
IMVM
Bioprocess Engineering
University of Karlsruhe
76131 Karlsruhe, Germany
- Balaji Prakash
bprakash@iitk.ac.in
Dept. of Biol. Sci. and Bio-Eng.
Indian Inst. of Tech.
Kanpur 208016, India
- Cristian Predescu
Dept. of Chemistry
University of California
Berkeley, CA 94720, USA
- Peter Pulay
pulay@uark.edu
Dept. of Chem. and Biochemistry
University of Arkansas
Fayetteville, AR 72701, USA
- Jagath C. Rajapakse
asjagath@ntu.edu.sg
Nanyang Tech. Univ.
School of Comput. Eng.
Block N4, No. 2a32
50 Nanyang Avenue
Singapore 639798
- Steven W. Rick
srick@uno.edu
Department of Chemistry
University of New Orleans
New Orleans, LA 70148, USA
- J.A. Robinson
Inst. of Org.Chem.
Univ. of Zurich
Winterthurerstrasse 190
8057 Zurich, Switzerland
- George D. Rose
grose@jhu.edu
T. C. Jenkins Dept. of Biophysics
The Johns Hopkins University
3400 N. Charles Street
Baltimore, MD 21218-2608, USA
- F. Rousseau
Switch Laboratory
VIB (Flemish Interuniv. Inst. Biotech.)
Vrije Univ. Brussel, Pleinlaan 2
1050 Brussels, Belgium
- Manfred Rudolph
cfr@uni-jena.de
Chemische Fakultät
Am Steiger 3
Friedrich-Schiller-Universität
D-07743 Jena, Germany
- Thomas Rush III
trush@wyeth.com
Wyeth Research
87 Cambridge Park Dr.
Cambridge, MA 02140, USA
- R.B. Russell
EMBL, Meyerhofstrasse 1
69117 Heidelberg, Germany
- A. M. Ruvinsky
anatoly.ruvinsky@algodign.com
Force Field Lab., Algodign, LLC
B. Sadovaya, 8
123379, Moscow, Russia.
- H. Bernard Schlegel
hbs@chem.wayne.edu
Dept. of Chemistry
Wayne State Univ.
Detroit, MI 48202, USA
- Tamar Schlick
schlick@nyu.edu
Dept. of Chemistry
New York Univ.
251 Mercer St.
New York, NY 10012, USA
- Gideon Schreiber
Dept. of Biol.Chem.
Weizmann Inst. of Sci.
Rehovot 76100, Israel
- Kim A. Sharp
sharpk@mail.med.upenn.edu
E.R. Johnson Res. Found.,
Dept. of Biochem. and BioPhys.
Univ. of Pennsylvania
3700 Hamilton Walk
Philadelphia, PA 19104-6049, USA
- Sheh-Yi Sheu
Faculty of Life Sciences
Institute of Biochemistry,
Institute of Bioinformatics, and
Structural Biology Program
National Yang-Ming University
Taipei 112, Taiwan
- Michael R. Shirts
Department of Chemistry
Stanford University
Stanford, CA 94305-5080, USA
- Jeremy C. Smith
biocomputing@
ivr.uni-heidelberg.de
IWR-Comput. Molec. Biophys.
Univ. of Heidelberg,
Im Neuenheimer Feld 368
69120 Heidelberg, Germany
- Vladimir Sobolev
vladimir.sobolev@weizmann.ac.il
Dept. Plant Sci.
Weizmann Inst. of Science
Rehovot 76100 Israel
- Jacob Sonne
Department of Chemistry
Technical University of Denmark
DK-2800 Lyngby, Denmark
- Maria Maddalena Sperotto
maria@cbs.dtu.dk
Biocentrum
The Tech. Univ. of Denmark
Kgs. Lyngby, Denmark
- Simeon D. Stoyanov
Unilever Research Vlaardingen
P.O. Box 114
3130 AC Vlaardingen,
The Netherlands
- Dimas Suárez
dimas@uniovi.es
Dept. de Quím. Fís. y Anal.
Univ. de Oviedo
Julián Clavería 8
33006 Oviedo, Spain
- S. Supple
Department of Chemistry
Imperial College London
London SW7 2AY, UK
- John O. Thomas
josh.thomas@mkem.uu.se
Dept. of Materials Chemistry
Box 538
Uppsala University
SE-75121 Uppsala, Sweden
- Thanh N. Truong
truong@chem.utah.edu
Dept. of Chemistry
Univ. of Utah
315 South 1400 East, Room 2020
Salt Lake City, UT 84112, USA
- Inaki Tunon
ignacio.tunon@uv.es
Dept. Química Física
Univ. de Valencia
46100 Burjassot, Spain
- G. Matthias Ullmann
matthias.ullmann@unibayreuth.de
IWR-Comput. Molec. Biophys.
Univ. of Heidelberg
Im Neuenheimer Feld 368
69120 Heidelberg, Germany
- Martin B. Ulmschneider
Dept. of Chem.
Univ. of Rome 'La Sapienza'
Piazzale Aldo Moro 5
I-00185 Roma, Italy

Alfred Ultsch
ultsch@
mathematik.uni-marburg.de
Data Bionics Res. Gr.,
Dept. of Comput. Sci.
Univ. of Marburg, Germany

Arjan van der Vaart
Dept. of Chem. & Chem. Biol.
Harvard University
Cambridge, MA 02138, USA
and
Institut de Science et
d'Ingénierie Supramoléculaires
Université Louis Pasteur
67000 Strasbourg, France

Wilfred F. van Gunsteren
wfvgn@igc.phys.chem.ethz.ch
Laboratory of Physical Chemistry
Swiss Federal Inst. of Technology
ETH-Hönggerberg
8093 Zurich, Switzerland

C. Vega
Departamento de Química Física
Facultad de Ciencias Químicas
Universidad Complutense
28040 Madrid, Spain

Carol A. Venanzia
venanzi@adm.njit.edu
Dept. of Chem. and Env. Sci.
New Jersey Inst. of Technology
323 King Blvd.
Newark, NJ 07102, USA

R.P. Verma
Dept. of Chem.
Pomona Coll.
Claremont, CA 91711, USA

Leslie Villalobos
Department of Chemistry
Univ. of Puerto Rico at Mayagüez
P.O. Box 9019
Mayagüez 00681-9019,
Puerto Rico

Gregory A. Voth
Dept. of Chemistry
Univ. of Utah
315 South 1400 East, Room 2020
Salt Lake City, UT 84112 USA

H. Wilczura-Wachnik
wilczura@alfa.chem.uw.edu.pl
The Fac. of Chem.
Warsaw Univ.
Pasteura 1 Street
02-093 Warsaw, Poland

Michael C. Wiener
mwiener@virginia.edu
Dept. of Molec. Physiol. and Biol.
Phys., Univ. of Virginia
Charlottesville, VA 22908-0736, USA

B. Windshügel
windshuegel@pharmazie.uni-halle.de
Dept. of Pharm.Chem.
Martin-Luther Univ.
Halle-Wittenberg
Wolfgang-Langenbeck-Str. 4
06120 Halle, Saale, Germany

Chung F. Wong
wongch@umsl.edu
Dept. of Chemistry and Biochem.
University of Missouri
St. Louis, MO 63121, USA

Guang Wu
hongguanglishibahao@yahoo.com
Compu. Mutation Project
Dream Sci. Tech Consulting Co. Ltd.
301, Building 12, Nanyou A-zone
Jiannan Road, Shenzhen
Guangdong Prov. 518054, China

Xiaojie Xu
xiaojxu@chem.pku.edu.cn
Coll. of Chem. and Mol. Engg.
Peking Univ.
Beijing, 100871, China

Bin Xue
Natl. Solid State Microstruct. Lab.
Inst. of Biophys. & Dept. of Phys.
Nanjing University
Nanjing 210093, PR China

Chang-Guo Zhan
zhan@uky.edu
Dept. of Pharm. Sci.
College of Pharmacy
Univ. Kentucky
725 Rose St.
Lexington, KY 40536, USA

Jun Zhuang
Zhuang1022@yahoo.com
Dept. of Optical Sci. and Engg.
Fudan University
Shanghai 200433, PR China

5. DISCLAIMER, COPYRIGHT, AND PUBLISHER INFORMATION

MMCC Results (ISSN 1061-6381), published by MMCC Results, 706 Sunny Lane, Orem, Utah 84058, is a private business independent of all software and hardware vendors, companies, government laboratories, universities, and other institutions whose products or publications may be cited herein. David D. Busath, M.D. is Professor of Physiology and Biophysics, Dept. of Physiology and Developmental Biology, Brigham Young University. Mention of a software product is for information purposes only and does not constitute an endorsement or recommendation by either MMCC Publishing or the authors of the paper cited. All product names are the trademarks or registered symbols of their respective organizations.

Copyright (c) 2005 by MMCC Publishing.

MMCC Results is published ten times per year, at the beginning of each month except January and August. For subscription information, please contact MMCC Publishing:

Editor:

David Busath, M.D.
MMCC Results
706 W. Sunny Lane
Orem, Utah 84058

Tel. (801) 422-8753
FAX (801) 422-0700
E-mail: mmcc@itsnet.com

Bruce Gelin, founder and editor of MMCC Results Volumes 1-6, is Editor Emeritus.

Associate Editor:

Thomas Cheatham, Depts. of Med. Chem. & of Pharmaceutics & Pharm. Chem., Univ. of Utah, Salt Lake City, UT.

Assistant Editors:

Alan C. Cheng, Pfizer Global R&D, Cambridge, MA

Anton Feenstra, Vrije Univ., Amsterdam, Netherlands

R. Nageswara Ramireddy, Genomik Design Pharmaceut. Pvt. Ltd., Hyderabad, India